

SEIFERT SURFACES IN THE 4-BALL

KYLE HAYDEN, SEUNGWON KIM, MAGGIE MILLER
JUNGHWAN PARK, AND ISAAC SUNDBERG

ABSTRACT. We answer a question of Livingston from 1982 by producing Seifert surfaces of the same genus for a knot in S^3 that do not become isotopic when their interiors are pushed into B^4 . In particular, we identify examples where the surfaces are not even topologically isotopic in B^4 , examples that are topologically but not smoothly isotopic, and examples of infinite families of surfaces that are distinct only up to isotopy rel. boundary. Our main proofs distinguish surfaces using the cobordism maps on Khovanov homology, and our calculations demonstrate the stability and computability of these maps under certain satellite operations.

1. INTRODUCTION

The following question was posed by Livingston [Liv82], generalizing Problem 1.20(C) in [Kir78, Kir97].

Question. *Let Σ_0 and Σ_1 be Seifert surfaces of equal genus for a knot K . After pushing the interiors of both surfaces into B^4 , are Σ_0 and Σ_1 isotopic in B^4 ?*

There are many known examples of knots bounding genus- g incompressible Seifert surfaces that are not isotopic in S^3 , dating back at least to work of Trotter [Tro75] (c.f. [Alf70]). However, as discussed below, most examples of such Seifert surfaces are known to become isotopic when their interiors are pushed into B^4 . This contrasts with the codimension-two setting, where there are a wealth of constructions that produce 4-dimensionally knotted surfaces in B^4 and other 4-manifolds (e.g. [Art26, Zee65, FS97]). In this light, Livingston's question asks if 4-dimensional knotting fundamentally requires all four dimensions. Our main results answer this question.

Theorem 1.1. *There exist minimal genus Seifert surfaces in S^3 with the same boundary that are not ambiently isotopic in B^4 .*

We provide a variety of counterexamples arising from three fundamentally distinct constructions, each highlighting different aspects of the problem; see §2. For a core pair of examples Σ_0 and Σ_1 , see Figure 1. Our main proofs distinguish surfaces up to smooth isotopy using the cobordism maps on Khovanov homology. These arguments expand on the computational techniques developed in [SS23, HS21], including the study of satellite operations (such as Whitehead doubling) on these cobordism maps. In particular, we are able to detect exotically knotted pairs of Seifert surfaces:

Theorem 1.2. *There exist infinitely many distinct pairs of minimal genus Seifert surfaces in S^3 that are topologically isotopic rel. boundary in B^4 yet are not smoothly ambiently isotopic in B^4 .*

KH is supported by NSF grant DMS-2114837. SK was supported by National Research Foundation of Korea (NRF) grants funded by the Korea government (MSIT) (No. 2020R1A5A1016126, 2022R1C1C2004559). MM is supported by a fellowship from the Clay Mathematics Institute and partially by a Stanford Science Fellowship. JP is partially supported by Samsung Science and Technology Foundation (SSTF-BA2102-02) and the POSCO TJ Park Science Fellowship.

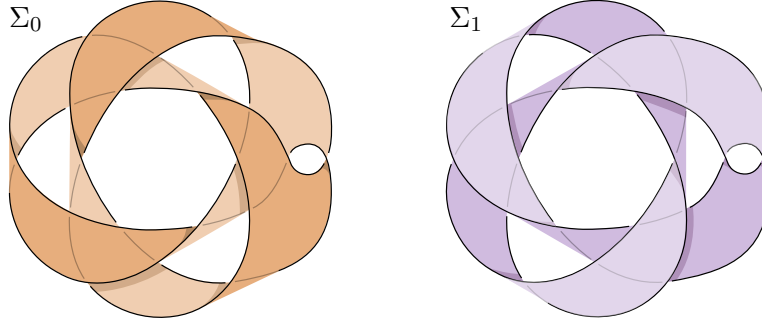


FIGURE 1. Two genus-1 Seifert surfaces Σ_0 (left) and Σ_1 (right) for the same knot K that are not isotopic even when their interiors are pushed into B^4 .

We also show that invariants of branched covers can distinguish Seifert surfaces up to isotopy in B^4 . Indeed, we have chosen the core examples Σ_0 and Σ_1 in such a way that they can also be distinguished using the intersection forms on their double branched covers; this implies that they are not even *topologically* isotopic in B^4 .

Theorem 1.3. *The Seifert surfaces Σ_0 and Σ_1 are not topologically isotopic in B^4 .*

We also consider the question of whether knots and links can bound infinitely many Seifert surfaces up to isotopy in B^4 . Constraints from normal surface theory imply that hyperbolic knots and links only bound finitely many Seifert surfaces of fixed genus up to isotopy rel. boundary in S^3 [SS64] (c.f. [Wil08] and [JPW14, Theorem 4]). Indeed, for any knot or link, there is an essentially unique way to generate infinite families of Seifert surfaces with the same genus and boundary, consisting of taking Haken sums of an initial Seifert surface with an incompressible torus in the knot or link complement. For knots and links with toroidal complements, the finiteness question is more subtle and depends on whether isotopies are taken rel. boundary. We show that this subtlety persists even up to isotopy through B^4 .

Theorem 1.4. *There exist links in S^3 that bound an infinite family of connected Seifert surfaces that are freely ambiently isotopic in S^3 yet are pairwise distinct up to smooth isotopy rel. boundary in B^4 .*

We distinguish the examples in Theorem 1.4 by studying the relative Seiberg-Witten invariants of their branched covers. We note that simpler obstructions suffice in the case of *disconnected* spanning surfaces. Indeed, as a point of contrast with Livingston's result [Liv82] (which states that *connected* Seifert surfaces for an unlink that have the same homeomorphism type are isotopic rel. boundary in B^4), we show that unlinks can bound infinitely many disconnected planar surfaces in S^3 up to topological isotopy rel. boundary in B^4 .

Theorem 1.5. *The 3-component unlink bounds infinitely many disconnected Seifert surfaces (each comprised of a disk and an annulus) that are distinct up to topological isotopy rel. boundary in B^4 .*

As mentioned above, our smooth obstructions hinge on new developments for calculating the cobordism maps on Khovanov homology. This reveals several surprising features of these cobordism maps, including their behavior under certain satellite constructions, as well as certain band sums that allow us to produce minimal genus Seifert surfaces. As an illustration of this, we note that Whitehead doubling plays particularly well with these cobordism maps, enabling us to prove the following general result:

Theorem 1.6. *If J is a nontrivial strongly quasipositive knot, then $\text{Wh}(J)$ bounds Seifert surfaces of equal genus that are topologically isotopic rel. boundary in B^4 yet are not smoothly ambiently isotopic in B^4 .*

It is interesting to compare these tools from Khovanov homology with their counterparts in Floer theory. While it seems likely that one could use the cobordism maps in knot Floer homology \widehat{HFK} to distinguish pairs of minimal genus Seifert surfaces (perhaps Σ_0 and Σ_1), these maps do not appear to be as amenable to direct calculation as the cobordism maps in Khovanov homology. Moreover, given that we use elementary methods to show that Σ_0 and Σ_1 are not even topologically isotopic, it would be more interesting to see the \widehat{HFK} cobordism maps used to distinguish a pair of Seifert surfaces that are topologically isotopic (or are at least not easily distinguished topologically). Distinguishing non-minimal genus Seifert surfaces appears to be especially subtle, given the close relationship between \widehat{HFK} and the Seifert genus; we discuss this further at the end of Section 3.

Organization. In Section 2, we provide an overview of our underlying constructions of Seifert surfaces. In Section 3, we perform our primary computations of Khovanov cobordism maps, distinguishing the core examples Σ_0 and Σ_1 , as well as their Whitehead doubles $\text{Wh}(\Sigma_0)$ and $\text{Wh}(\Sigma_1)$. We generalize aspects of these concrete calculations by proving Theorem 1.6 in §3.4. In §3.5, we modify the earlier examples to produce minimal genus Seifert surfaces that are not smoothly ambiently isotopic, concluding the proof of Theorem 1.2. Finally, in Section 4, we turn to obstructions arising from branched covers, proving Theorems 1.3 and 1.4.

Conventions. In this paper, we will always specify whether results hold in the smooth or locally flat category, as we work in each at different times. We will forever refer to the surfaces in Figure 1 as Σ_0 and Σ_1 , and their boundary as K . For convenience, we work with Khovanov homology over \mathbb{Z}_2 coefficients.

Acknowledgements. Some of the authors learned of the motivating question of this paper from Peter Teichner in spring 2021; we thank him for many interesting conversations and helpful comments. This project came about during the “Braids in Low-Dimensional Topology” conference at ICERM in April 2022. We thank the organizers for putting together an engaging conference.

2. CONSTRUCTIONS AND COUNTEREXAMPLES

For context, we begin by revisiting some of the historical constructions of pairs of distinct Seifert surfaces with the same genus and boundary in §2.1. We then present

our three main constructions in §2.2-2.4. These sections state more precise versions of the results from §1, whose proofs will then be given in §3-§4.

2.1. Historical constructions. There are many known examples of knots bounding genus- g incompressible Seifert surfaces that are not isotopic in S^3 (e.g. [Alf70, AS70, Dai73, Lyo74, Tro75, Eis77, Par78, Gab86, Kob89, Kak91, HJS13, Vaf15]). Most of these examples of distinct Seifert surfaces are known to become isotopic when their interiors are pushed into B^4 . The pairs of surfaces of [Alf70, AS70, Dai73] are constructed by choosing one of two tubes to include in the surface that become isotopic when pushed deeper into B^4 (see [Rol76, p123]); the pretzel surfaces of [Tro75, Par78] (c.f. [Kob92]) were shown to be isotopic in B^4 by Livingston [Liv82, Section 6], who also showed that any connected, genus- g Seifert surfaces for an unlink become isotopic in B^4 ; the surface families in [Eis77, Kak91] are obtained by twisting a surface many times about a satellite torus, which can be undone by isotopy in B^4 (see Proposition 2.6); the examples of [Gab86, Kob89, HJS13, Vaf15] arise from a Murasugi sum construction and are isotopic in B^4 via an isotopy involving pushing the plumbing region deeper into B^4 (see [Vaf15, Remark 3.1]).

However, for one fairly well-known family of examples due to Lyon [Lyo74], there is no clear isotopy between the surfaces even when they are pushed into B^4 . Lyon's examples are genus-1 Seifert surfaces obtained by attaching a common band to each of two different choices of annuli with the same boundary. Together, those underlying annuli form the standard torus in S^3 , with their common boundary given by an unoriented $(6, -8)$ torus link. Lyon distinguished these surfaces in S^3 via the fundamental groups of their complements; Altman [Alt12] studied the same surfaces and showed that they are also distinguished by the sutured Floer polytopes of their complements.

2.2. Cutting up closed surfaces. Our first approach is based on a generalization of Lyon's construction, and is animated by a simple observation: A link $L \subset S^3$ bounds a pair of genus- g Seifert surfaces with disjoint interiors if and only if L lies on a closed genus- $2g$ surface in S^3 and separates it into a pair of genus- g surfaces.

Example 2.1. The core examples Σ_0 and Σ_1 from Figure 1 provide pair of genus-1 Seifert surfaces for a twisted Whitehead double K of the left-handed trefoil. As illustrated in Figure 2, the union of Σ_0 and Σ_1 is a standard, closed, genus-2 surface in S^3 . (Here the underlying annuli are bounded by an unoriented $(4, -6)$ torus link, and we attach a common band to the right-hand side of each annulus.)

We distinguish Σ_0 and Σ_1 using Khovanov homology in the proof of Proposition 3.1. In Theorem 4.1, we further distinguish Σ_0 and Σ_1 up to topological isotopy by showing their double branched covers are not homeomorphic.

Example 2.2. A second example of this form is shown in Figure 3, which depicts a genus-4 surface cut into a pair of genus-2 Seifert surfaces for the Whitehead double of the right-handed trefoil knot; after isotopy, these are redrawn in Figure 7. These examples turn out to be topologically isotopic yet smoothly distinct (by Theorem 1.6).

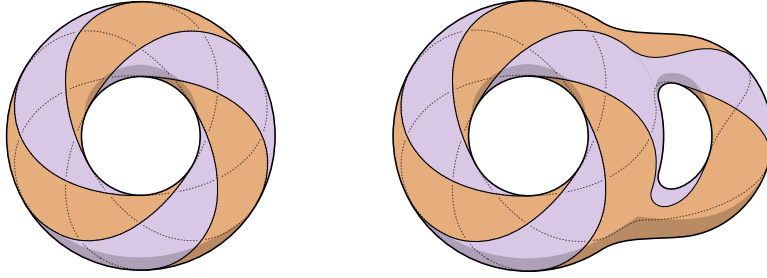


FIGURE 2. Left: two annuli bounded by an unoriented $(4, -6)$ torus link whose union is a standard torus. Right: the surfaces Σ_0, Σ_1 , whose union is a standard genus-2 surface.

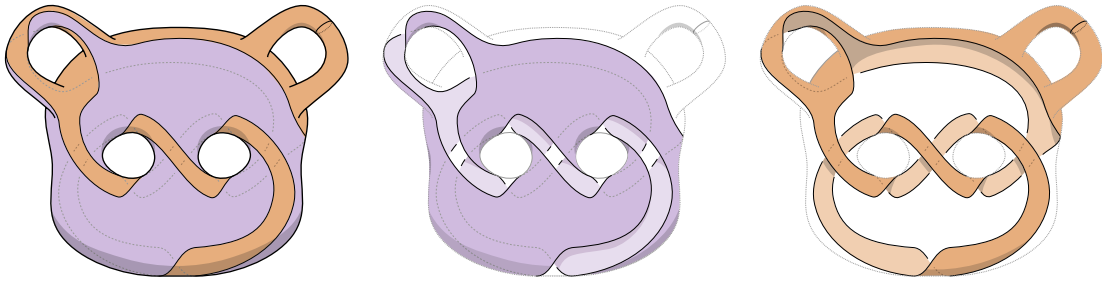


FIGURE 3. Cutting a standard genus-4 surface into a pair of genus-2 Seifert surfaces for the Whitehead double of the right-handed trefoil.

2.3. Haken sums and torus twists. Using normal surface theory, Schubert-Soltsien [SS64] showed that non-satellite knots in S^3 have only finitely many Seifert surfaces of fixed genus up to isotopy rel. boundary (known as *strong equivalence*), and the same holds for links with atoroidal complements [JPW14, Theorem 4]. In contrast, satellite knots and links may have infinitely many Seifert surfaces up to isotopy rel. boundary in S^3 . In this case, infinite families may be generated by fixing an initial Seifert surface S and taking Haken sums of S with copies of an incompressible torus T in the knot or link complement $S^3 \setminus \partial S$.

An important example of this operation is given by *torus twists*, defined as follows: Suppose that S intersects T transversely along a collection of essential curves in T , all of which will necessarily be parallel. Dehn's lemma implies that T bounds a solid torus V in S^3 , so we may choose coordinates identifying T with $T^2 = S^1 \times S^1$ such that each curve $S^1 \times \{\text{pt}\}$ bounds a disk in V . (The other coordinate direction $\{\text{pt}\} \times S^1$ may be chosen freely, e.g., to be nullhomologous in $S^3 \setminus \mathring{V}$, or to coincide with the curves $S \cap T$.) Extend these coordinates to a neighborhood $T^2 \times [0, 1]$ of $T = T^2 \times \{1/2\}$. We define a *meridional twist along T* to be a diffeomorphism that is defined on $T^2 \times [0, 1]$ by $(x, y, t) \mapsto (x + 2\pi t, y, t)$ and by the identity on the rest of S^3 ; a *longitudinal twist* is defined analogously.

For a schematic depiction of the effect of a meridional twist on S , see Figure 4. It is straightforward to show that Seifert surfaces related by torus twists are freely isotopic

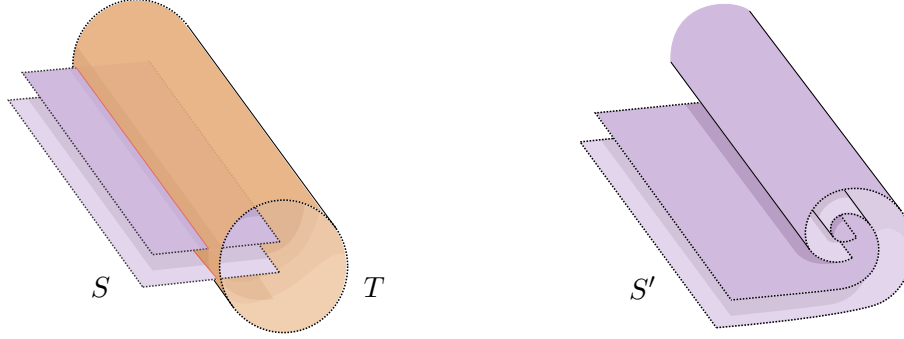


FIGURE 4. Twisting a surface S along a torus T producing a new surface S' , where T intersects S transversely in its interior.

in S^3 . (The isotopy can be constructed directly using the fact that T bounds a solid torus in S^3 , c.f. [Eis77, p332].) However, they need not be isotopic rel. boundary.

Example 2.3. Consider the surface S_0 in Figure 5; it is constructed by taking a pair of interlocked annuli bounded by an unoriented $(4, 8)$ -torus link, then joining these annuli by a twisted band. Its boundary $L = \partial S_0$ is a 3-component link, and the link complement $S^3 \setminus L$ contains an essential torus T meeting S_0 transversely along a pair of simple closed curves. Twisting S_0 along T yields an infinite family of surfaces S_n for L . In Section 4, we will show that the Seifert surfaces S_n are not smoothly isotopic rel. boundary in B^4 (proving Theorem 1.4).

2.4. Satellite surfaces. Satellite operations provide an important construction of knots in 3-manifolds, and analogous constructions can be applied to Seifert surfaces. Let L be a link in S^3 whose complement $S^3 \setminus L$ contains an incompressible torus T . We say that a spanning surface $S \subset S^3$ for L is a *satellite with respect to T* if T is transverse to S and bounds a solid torus V such that: (i) $L = \partial S$ lies in V , and (ii) S meets $S^3 \setminus \mathring{V}$ in a collection of parallel push-offs of a fixed surface F bounded by a longitude on ∂V . Technically, we allow F to be empty. Note that if F is nonempty, then it must have positive genus, otherwise the torus T would be compressible.

In practice, we will construct such surfaces by fixing an initial Seifert surface F for a knot J and a tubular neighborhood V of $J = \partial F$, then choosing n parallel push-offs of F and gluing them to a “pattern surface” lying entirely in V (for examples, see Figure 6). The resulting surface S is a satellite with respect to $T = \partial V$.

Example 2.4. Let J denote the right-handed trefoil, and let $\text{Wh}(J)$ denote its positively clasped, untwisted Whitehead double, illustrated on the left side of Figure 7. The middle of Figure 7 depicts a genus-2 satellite Seifert surface for $\text{Wh}(J)$ built from two copies of the standard fiber surface for J . We can produce a second genus-2 Seifert surface for $\text{Wh}(J)$ by stabilizing the standard genus-1 Seifert surface for $\text{Wh}(J)$, as shown on the right side of Figure 7. (Technically, this is also a satellite with respect to the natural torus, where the subsurface F is empty.) We will distinguish these surfaces up

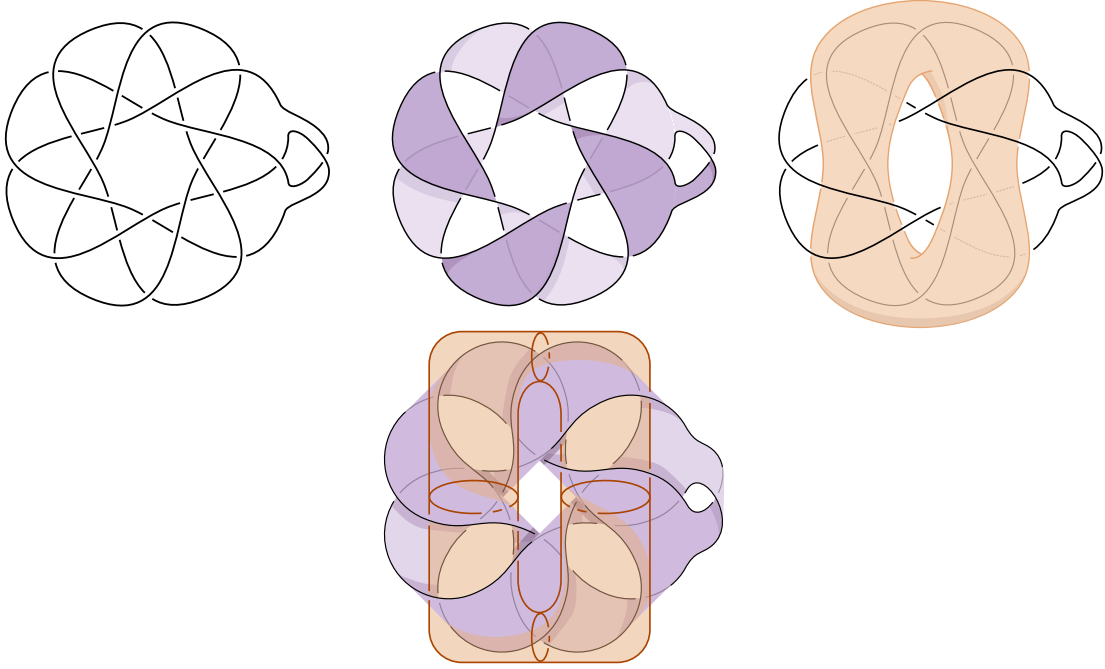


FIGURE 5. Twisting the top middle surface about the torus featured in the top right yields an infinite family of Seifert surfaces for a 3-component link that are not isotopic rel. boundary. See Example 2.3 and Theorem 1.4.

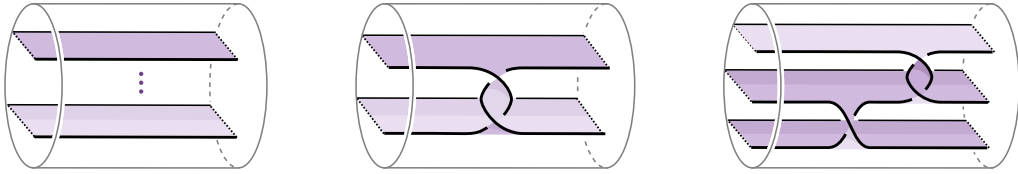


FIGURE 6. From left to right, satellite pattern surfaces bounded by the n -copy pattern, the positive Whitehead pattern, and the Mazur pattern.

to smooth isotopy in B^4 using Khovanov homology in §3.4. However, by Theorem 2.7 below, these surfaces turn out to be topologically isotopic rel. boundary in B^4 .

Continuing the analogy with satellite knots, we say that the *wrapping number* of a satellite surface S with respect to a torus T is the number of components in $S \cap T$, and the *winding number* is the absolute value of the signed count of components in $S \cap T$ as a collection of oriented curves (i.e., the divisibility of $[S \cap T]$ in $H_1(T)$).

Our final construction generalizes Example 2.4:

Proposition 2.5. *Let $S \subset S^3$ be a connected, positive-genus Seifert surface for a link L , and suppose that S is a satellite with respect to an incompressible torus in $S^3 \setminus L$. If the wrapping number of S exceeds the winding number, then L has another Seifert surface of genus strictly less than $g(S)$.*

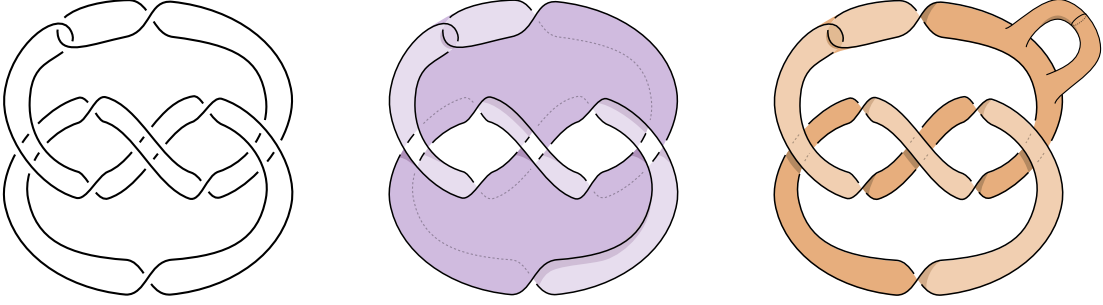


FIGURE 7. Left: $\text{Wh}(J)$, where J is the right-handed trefoil. Middle: a genus-2 surface obtained by Whitehead doubling the genus-1 Seifert surface for J . Right: a genus-2 surface obtained by adding a trivial tube to a genus-1 Seifert surface for $\text{Wh}(J)$.

Proof. Let $T \subset S^3 \setminus L$ be the incompressible torus with respect to which S is a satellite, and let r and w denote the wrapping and winding numbers of S with respect to T , respectively. By definition, S meets one of the components of $S^3 \setminus T$ in r copies of a subsurface F . Since $r > w \geq 0$, F must be a nonempty surface with $g(F) \geq 1$. The torus T intersects S in r parallel curves and, since $r > w$, there must be at least one pair of adjacent curves C_{\pm} whose orientations (induced by those on S and T) are opposite. These curves cobound an annulus $A \subset T$ whose interior is disjoint from S , so we may construct a new Seifert surface S' for L by removing the two parallel copies of F bounded by C_{\pm} and gluing in the annulus A . Observe that

$$g(S') = g(S) - 2g(F) + 1 < g(S),$$

where the $+1$ term in the first equality appears because A joins two components of a connected surface. \square

Proposition 2.5 gives rise to a construction of pairs of equal-genus satellite Seifert surfaces for many satellite knots: an initial satellite surface S , and a satellite surface of lower wrapping number obtained from the lower-genus surface S' (as constructed in the proof of Proposition 2.5) by stabilizing it until it has the same genus as S . The primary situation that we consider involves Whitehead doubling, as illustrated by Example 2.4 and discussed further in §2.4.1.

Before focusing on Whitehead doubles, we pause to consider the effect of torus twisting (as discussed in §2.3) on satellite surfaces. As demonstrated in [Eis77, Kak91], applying torus twists to a satellite Seifert surface can yield infinite families of Seifert surfaces that are distinct up to isotopy rel. boundary in S^3 . However, the next proposition shows that such surfaces are smoothly isotopic rel. boundary in B^4 .

Proposition 2.6. *Let S be a Seifert surface in S^3 that is a satellite with respect to a torus T . If S' is obtained from S by meridional twists along T , then S and S' are smoothly isotopic rel. boundary in B^4 .*

Proof. By definition, the torus T bounds a solid torus $V \subset S^3$ that contains the link $L = \partial S$, and S meets $S^3 \setminus \mathring{V}$ in sheets consisting of parallel copies of a fixed subsurface

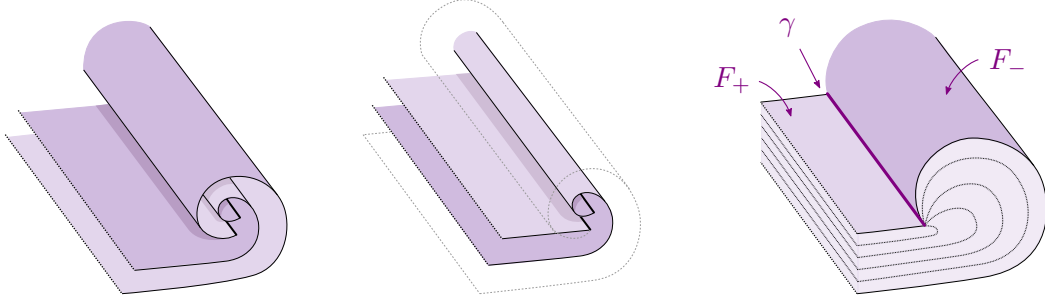


FIGURE 8. Left: The surface S' , obtained from a satellite surface S by twisting along the satellite torus. Middle: the intermediary surface \hat{S} from the proof of Proposition 2.6. Right: the surfaces F_+ and F_- cobounding a product in S^3 .

F . The surface S' is obtained from S by twisting these sheets around the $T = \partial V$ as depicted on the left side of Figure 8 (or its mirror through a horizontal plane).

As an intermediate step, we consider a surface \hat{S} as depicted in the middle of Figure 8, obtained from S' by removing a twist from an outermost sheet; note that this has the effect of changing which sheet is on top. Up to isotopy rel. boundary, we may assume that \hat{S} and S' coincide everywhere except for the interiors of two subsurfaces $F_- \subset S'$ and $F_+ \subset \hat{S}$ as illustrated on the right side of Figure 8. Moreover, these subsurfaces F_{\pm} are each isotopic to the original subsurface F , and their common boundary is a curve γ that is isotopic to ∂F .

There is a simple isotopy from F_- to F_+ rel. γ in S^3 . By pushing the interiors of the intermediate surfaces into B^4 , we obtain an isotopy from S' to \hat{S} rel. boundary in B^4 . By repeating this argument (such that the total number of iterations is $|S \cap T|$), we construct an isotopy from S' to S . \square

2.4.1. Whitehead doubles. Let S be a Seifert surface for a knot J . The *positive Whitehead double* $\text{Wh}(S)$ of S is a Seifert surface for the positive Whitehead double $\text{Wh}(J)$ of J obtained by joining two parallel copies of S (of opposite orientations) via a positively twisted band. Figure 9 depicts the positive Whitehead double of the surface Σ_1 .

A key motivation for this section is the following theorem of Conway and Powell.

Theorem 2.7 ([CP20, Theorem 1.9]). *Any pushed-in Seifert surfaces of the same genus for a knot with Alexander polynomial 1 are topologically isotopic rel. boundary in B^4 .*

Returning to the main examples Σ_0 and Σ_1 from Figure 1, Theorem 2.7 implies that $\text{Wh}(\Sigma_0)$ and $\text{Wh}(\Sigma_1)$ are topologically isotopic rel. boundary, even though Σ_0 and Σ_1 are not topologically isotopic (as we show in Theorem 4.1). In Section 3, we use Khovanov homology to obstruct $\text{Wh}(\Sigma_0)$ and $\text{Wh}(\Sigma_1)$ from being smoothly isotopic.

Remark 2.8. As a technical point, we note that an isotopy between two Seifert surfaces S_0 and S_1 for a knot J induces an isotopy between the doubles $\text{Wh}(S_0)$ and $\text{Wh}(S_1)$. However, the doubled surfaces need not be isotopic rel. boundary, even if S_0 and S_1 are isotopic rel. boundary. Fortunately, for our purposes, Proposition 2.6 ensures that positive Whitehead doubles of surfaces are indeed well-defined up to isotopy rel. boundary

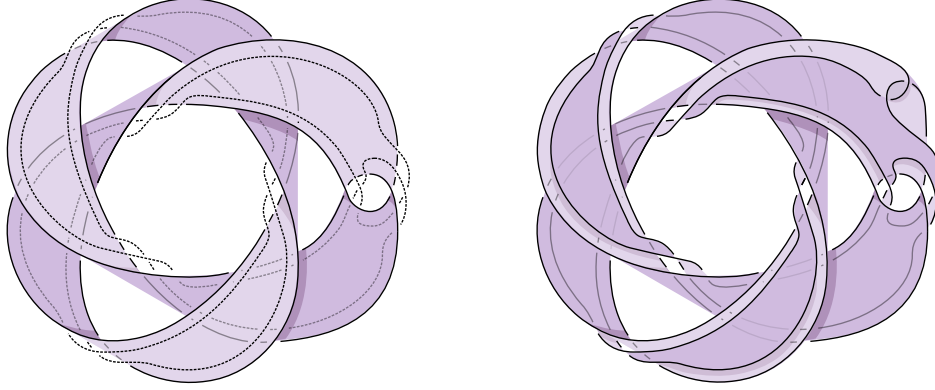


FIGURE 9. Left: the Seifert pushoff of the knot K and the surface Σ_1 . Right: the positive Whitehead doubled surface $\text{Wh}(\Sigma_1)$.

in B^4 . Indeed, in order to obtain a positive Whitehead double of a surface S , we first have to choose an annulus A between ∂S and the boundary of a tubular neighborhood N of ∂S . We isotope S rel. boundary to agree with A in N and then double S and attach a band to obtain $\text{Wh}(S)$. If we use a different annulus A' that twists one more time about the meridian of N , then the resulting surface will differ from the original by a twist along the satellite torus ∂N . (Or in other words, $\text{Wh}(S)$ is defined unambiguously outside of a tubular neighborhood of its boundary, up to isotopy fixing the Whitehead satellite torus T setwise.)

2.4.2. Extending smooth symmetries. The goal of this subsection is to establish the following proposition, which will play a key role in showing that $\text{Wh}(\Sigma_0)$ and $\text{Wh}(\Sigma_1)$ are not equivalent under any smooth ambient isotopy (and not merely isotopies that fix the boundary). In the following proposition, recall that K and Σ_1 are specifically as in Figure 1.

Proposition 2.9. *Any diffeomorphism of S^3 that fixes K (resp. $\text{Wh}(K)$) setwise extends to a diffeomorphism of B^4 that fixes Σ_1 (resp. $\text{Wh}(\Sigma_1)$) setwise.*

Given a knot $J \subset S^3$, let $\text{Diff}(S^3, J)$ denote the group of diffeomorphisms of S^3 that fix J setwise. The symmetry group of J , denoted $\text{Sym}(J)$, is the quotient of the group $\text{Diff}(S^3, J)$ by $\text{Diff}_0(S^3, J)$, the normal subgroup of diffeomorphisms that are isotopic to the identity through diffeomorphisms of the pair (S^3, J) . The following lemma reduces Proposition 2.9 to an analysis of the discrete, finitely generated group $\text{Sym}(J)$ instead of the infinite-dimensional group $\text{Diff}(S^3, J)$.

Lemma 2.10. *Let $S \subset B^4$ be a smooth, properly embedded surface bounded by a knot $J \subset S^3$. If every element of $\text{Sym}(J)$ has a representative in $\text{Diff}(S^3, J)$ that extends to a diffeomorphism of (B^4, S) , then every diffeomorphism of (S^3, J) extends to a diffeomorphism of (B^4, S) .*

Proof. Let f be any diffeomorphism of the pair (S^3, J) . By hypothesis, there exists $g \in \text{Diff}(S^3, J)$ representing the same element of $\text{Sym}(J)$ such that g extends to a

diffeomorphism of (B^4, S) . To show that f extends to a diffeomorphism of (B^4, S) , it then suffices to show that $g^{-1} \circ f$ extends, for we may then compose with the extension of g to obtain an extension of f .

The equivalence of f and g in $\text{Sym}(J)$ implies that these maps are isotopic through diffeomorphisms of (S^3, J) . This implies that $g^{-1} \circ f$ is isotopic to the identity through diffeomorphisms of (S^3, J) . Thus, it suffices to prove that every element of $\text{Diff}_0(S^3, J)$ extends to a diffeomorphism of (B^4, S) .

For notational convenience, view $B^4 \setminus \{pt\}$ as $S^3 \times (-\infty, 1]$ and choose an isotopy $\psi_t : B^4 \rightarrow B^4$ (rel. ∂B^4) that straightens a collar neighborhood of S , i.e. where $\psi_0 = \text{id}$ and $\psi_1(S) \cap (S^3 \times (0, 1]) = J \times (0, 1]$. Given an element $h \in \text{Diff}_0(S^3, J)$, choose an isotopy h_t with $h_0 = \text{id}$ and $h_1 = h$. Now define $H_t : B^4 \rightarrow B^4$ by $H_t(x, r) = (h_{rt}(x), r)$ for all $(x, r) \in S^3 \times (0, 1]$ and by the identity on the rest of B^4 . Then $\psi_t^{-1} \circ H_t \circ \psi_t$ is an isotopy from the identity at $t = 0$ to a new diffeomorphism at $t = 1$ that extends h to all of B^4 and maps S to itself, as desired. \square

Proof of Proposition 2.9. We will write the proof just for $\text{Wh}(\Sigma_1)$; the proof for Σ_1 is implicit and strictly easier. The knot K is itself the -6 -framed positive Whitehead double of the left-handed trefoil. Thus, the complement of $\text{Wh}(K)$ admits a JSJ decomposition consisting of the following pieces:

- (1) M_1 , a left-handed trefoil complement,
- (2) M_2 , the complement of the -6 -framed positive Whitehead link,
- (3) M_3 , the complement of the standard Whitehead link.

Any self-homeomorphism f of $(S^3, \text{Wh}(K))$ must fix this decomposition up to isotopy. The map f is determined up to isotopy by an automorphism of each M_i that fixes the ordering of its boundary components, up to twists about the tori boundary of each M_i .

Observe that M_2 and M_3 are homeomorphic as 3-manifolds (although not by a homeomorphism preserving meridians of the associated links). Both these manifolds have automorphism group D_4 (see [HW92, Table 2]), but this includes a map that switches the two boundary components. Quotienting by this map, the automorphism groups of M_2 and M_3 fixing each boundary component setwise are $\mathbb{Z}_2 \oplus \mathbb{Z}_2$.

We temporarily project $\text{Wh}(\Sigma_1)$ back into $S^3 = \partial B^4$ and consider its intersections with M_1, M_2 , and M_3 . Note that $\text{Wh}(\Sigma_1)$ does not intersect M_1 . We illustrate the intersections of $\text{Wh}(\Sigma_1)$ with M_2 and M_3 in Figure 10. The automorphism group of M_2 fixing boundary components is generated in Figure 10 (left) by 180° rotation about a horizontal axis and 180° rotation about a circular axis in the plane of the drawing. Both of these maps fix $\text{Wh}(\Sigma_1) \cap M_2$ setwise. The part of the automorphism group of M_3 preserving both boundary components is similarly generated in Figure 10 (right) by rotation about a horizontal axis and rotation about a circular axis in the plane of the drawing. Again, both of these maps fix $\text{Wh}(\Sigma_1) \cap M_3$ setwise.

So far, we have seen that automorphisms of M_2 and M_3 are isotopic to ones that fix the portion of $\text{Wh}(\Sigma_1)$ inside M_2 or M_3 setwise (even in S^3). Thus, we need only consider twists about the JSJ tori. Moreover, since $\text{Wh}(\Sigma_1)$ does not intersect the torus separating M_1 and M_2 , we need only consider the tori that cobound M_3 . We now push the interior of $\text{Wh}(\Sigma_1)$ slightly back into B^4 . One of these tori is the boundary of

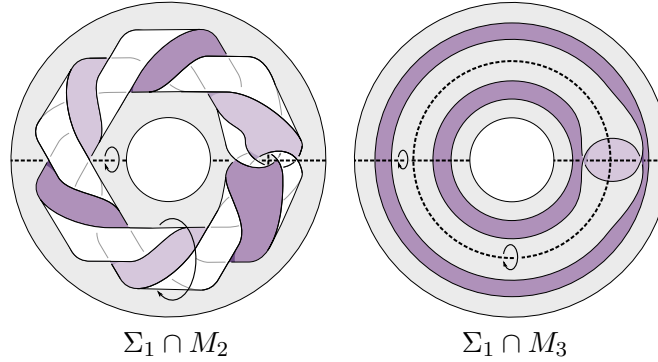


FIGURE 10. Intersections of $\text{Wh}(\Sigma_1)$ with the JSJ pieces M_2 and M_3 . The manifold M_2 is the complement of the -6 -framed positive Whitehead link; Σ_1 intersects M_2 in two components that twist about the “inner” boundary. The manifold M_3 is the complement of the usual Whitehead link; here one boundary is filled to indicate $\text{Wh}(K)$.

a tubular neighborhood of $\text{Wh}(K)$; twists about this torus can be extended over this solid torus taking $\text{Wh}(K)$ to be a fixed core. The other torus is the Whitehead satellite torus. By Proposition 2.6, twists about this torus preserves $\text{Wh}(\Sigma_1)$ up to isotopy rel. boundary in B^4 . \square

3. OBSTRUCTIONS FROM KHOVANOV HOMOLOGY

3.1. Khovanov preliminaries. Khovanov homology is known to be functorial for link cobordisms in $\mathbb{R}^3 \times [0, 1]$, in the sense that a smooth, oriented, properly embedded cobordism $S \subset \mathbb{R}^3 \times [0, 1]$ between links L_0 and L_1 induces a diagrammatically-defined \mathbb{Z}_2 -linear map on Khovanov homology $\text{Kh}(S) : \text{Kh}(L_0) \rightarrow \text{Kh}(L_1)$ that is invariant under smooth isotopy of S rel. boundary [Kho00, Jac04, BN05, Kho06]. We make note of an important extension of this invariant from [MWW22, Lemma 4.7] and [LS22, Proposition 3.7], where it is proven that a (possibly non-orientable) link cobordism in $S^3 \times [0, 1]$ induces a map on Khovanov homology that is invariant under diffeomorphism of $S^3 \times [0, 1]$ that restricts to the identity on the boundary.

The Khovanov functor can be adapted to the setting of surfaces in B^4 . To that end, suppose $S_0, S_1 \subset B^4$ are surfaces bounded by the same link $L \subset S^3$. Any boundary-preserving diffeomorphism of B^4 carrying S_0 to S_1 can be taken to fix a small open ball in the complement of the surfaces (via an isotopy supported far from the surfaces). This induces a diffeomorphism of link cobordisms in $S^3 \times [0, 1]$. Thus, to distinguish the surfaces S_0 and S_1 in B^4 , it suffices to distinguish the link cobordisms $L \rightarrow \emptyset$ they induce in $S^3 \times [0, 1]$, or equivalently, to distinguish the maps $\text{Kh}(L) \rightarrow \mathbb{Z}_2$ they induce on Khovanov homology.

Previous work has proven the efficacy of this technique by showing that the maps on Khovanov homology distinguish many families of surfaces in B^4 up to diffeomorphism rel. boundary, including exotic examples [HS21, LS22, SS23]. Moreover, the approach in [HS21] demonstrates the computability of such maps: by carefully choosing a cycle

$\psi \in \mathcal{CKh}(L)$ from the Khovanov chain complex of L , we can control the complexity of calculating the induced chain maps $\mathcal{CKh}(S_0)(\psi)$ and $\mathcal{CKh}(S_1)(\psi)$. Moreover, the calculations in this paper only require a subset of the Morse and Reidemeister induced chain maps (c.f. [HS21, Tables 1-2]), tailored to x -labeled smoothings with \mathbb{Z}_2 coefficients.

3.2. Main example computation. To motivate the main obstruction from Khovanov homology in Theorem 1.2, we begin by distinguishing the maps on Khovanov homology induced by Σ_0 and Σ_1 . In combination with Proposition 2.9 (c.f. Corollary 3.8), this proves Theorem 1.1 in the smooth setting. Moreover, the computations of $\mathcal{CKh}(\Sigma_0)$ and $\mathcal{CKh}(\Sigma_1)$ set the groundwork from which we distinguish the maps induced by $\text{Wh}(\Sigma_0)$ and $\text{Wh}(\Sigma_1)$.

Proposition 3.1. *The Seifert surfaces Σ_0 and Σ_1 induce distinct maps on Khovanov homology, distinguished by a given cycle $\phi \in \mathcal{CKh}(K)$, and hence are not related by any diffeomorphism of B^4 that restricts to the identity on ∂B^4 (and in particular are not smoothly isotopic rel. boundary in B^4).*

Proof. A smoothing of K is given on the top-right of Figure 11, and a straightforward calculation shows that x -labeling each component produces a cycle $\phi \in \mathcal{CKh}(K)$ in the Khovanov chain complex (0-smoothed crossings are indicated by a gray band on ϕ and connect distinct x -labeled components). We immediately note that the map on the Khovanov chain complex induced by Σ_0 satisfies $\mathcal{CKh}(\Sigma_0)(\phi) = 0$, as one can find many band moves describing Σ_0 whose induced map merges distinct x -labeled components of ϕ . A complementary calculation for the chain map induced by Σ_1 is given in Figure 11 (completed after capping off the remaining unknots), and shows $\mathcal{CKh}(\Sigma_1)(\phi) = 1$. We conclude that ϕ distinguishes the maps induced by these surfaces, implying that there is no diffeomorphism of B^4 restricting to the identity on ∂B^4 that sends Σ_0 to Σ_1 . \square

Remark 3.2. The movie of Σ_1 that we chose in Figure 11 localizes the induced chain map on Khovanov homology. In particular, Σ_1 can be decomposed into a collection of *band twists* \times and *band crossings* \bowtie , with which we compute $\mathcal{CKh}(\Sigma_1)$ as a collection of isolated chain maps on the corresponding boundary tangles (c.f. [Kho02, BN05]). The chosen tangle decomposition of K sheds light on how we chose a cycle: within each tangle, ϕ has a consistent labeled smoothing, where band twists have oriented smoothings, band crossings have nonoriented smoothings, and only x labels are used throughout. In the next section, we show that this localization is, in some sense, stable under the process of Whitehead doubling from Section 2.4.

3.3. Whitehead doubling and Khovanov homology. We now distinguish the maps on Khovanov homology induced by $\text{Wh}(\Sigma_0)$ and $\text{Wh}(\Sigma_1)$. Motivated by the previous section: we decompose $\text{Wh}(K)$ into a collection of tangles which reflect the local behavior of $\text{Wh}(\Sigma_1)$, we choose a cycle $\Phi \in \mathcal{CKh}(\text{Wh}(K))$ by choosing labeled smoothings for each tangle, and finally, we calculate the induced maps on Φ as a collection of tangle maps.

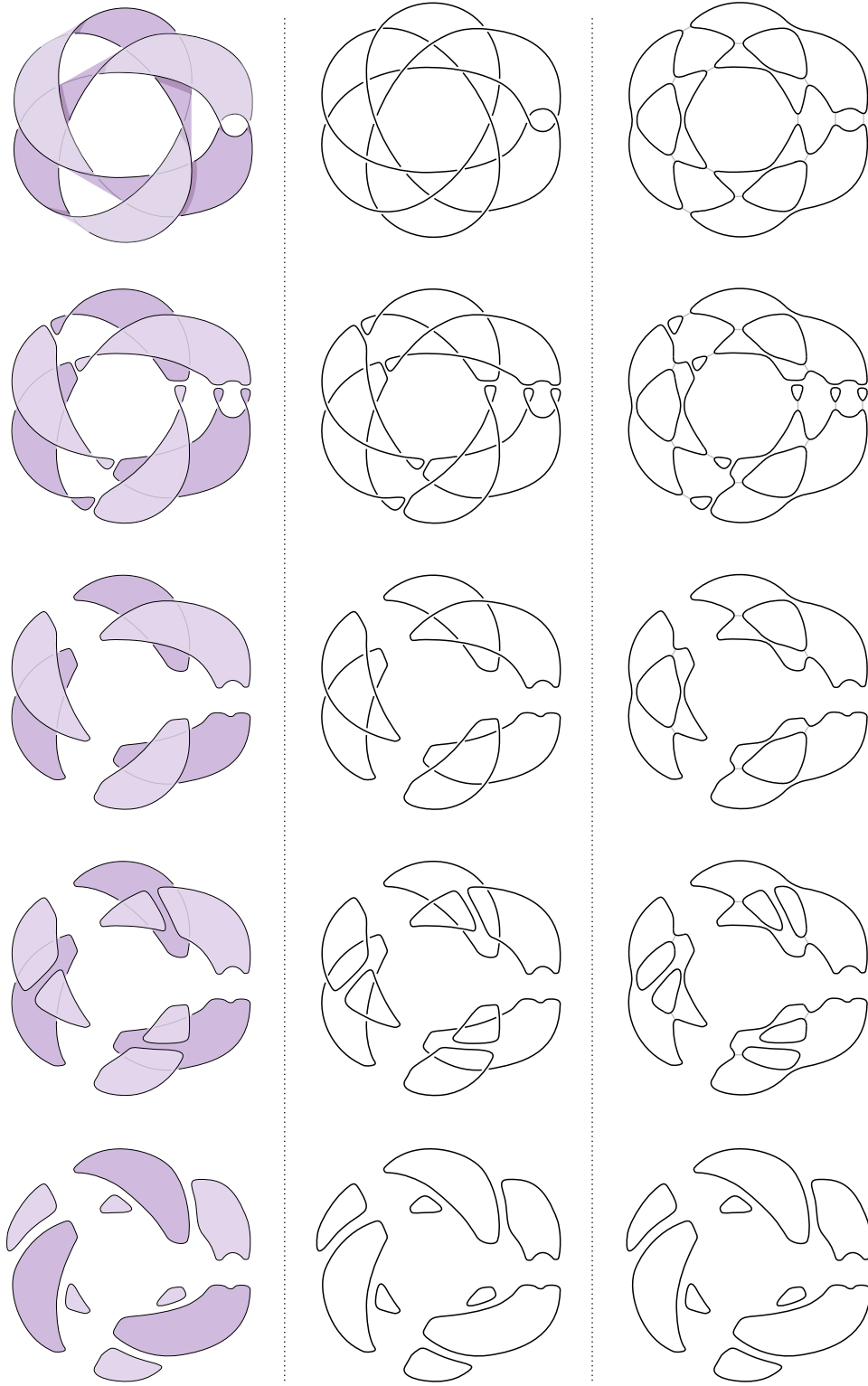


FIGURE 11. Left: the surface Σ_1 as it is dipped into B^4 . Middle: the corresponding movie. Right: the effect of each move on ϕ , with all smoothings x -labeled.

Theorem 3.3. *The surfaces $\text{Wh}(\Sigma_0)$ and $\text{Wh}(\Sigma_1)$ induce distinct maps on Khovanov homology, distinguished by a given cycle $\Phi \in \mathcal{CKh}(\text{Wh}(K))$, and hence, are not related by a diffeomorphism of B^4 restricting to the identity on ∂B^4 (and in particular are not smoothly isotopic rel. boundary in B^4).*

Theorem 3.3 implies Theorem 1.2 in the finite case and up to smooth equivalence rel. boundary (see the discussion in Section 2.4.1 and, in particular, Theorem 2.7).

Proof of Theorem 3.3. To begin, observe that $\text{Wh}(\Sigma_1)$ exhibits three types of local behavior, illustrated in the first row of Figure 12: *big twists*, *big crossings*, and a single *Whitehead clasp*. The boundary of each is illustrated in the second row as a tangle in $\text{Wh}(K)$, decorated with band moves to reflect the local behavior of the surface $\text{Wh}(\Sigma_1)$. In the third row, we choose a labeled smoothing for each tangle. We extend to a labeled smoothing $\Phi \in \mathcal{CKh}(\text{Wh}(K))$ by noting that the strands connecting any two tangles are consistently x -labeled.

We may dip $\text{Wh}(\Sigma_1)$ into $S^3 \times [0, 1]$ to produce a movie consisting of two stages: first, the band moves within each tangle, followed by a sequence of Reidemeister moves that simplify each tangle; second, a sequence of Morse deaths that cap off the resulting crossingless unlink. The first stage is localized within each tangle in Figure 12, so the map it induces is localized to labeled smoothings of that tangle. When applied to the relevant labeled smoothings for a big twist, big crossing, and Whitehead clasp, we obtain the final row of Figure 12. Overall, the first stage maps Φ to the all x -labeled smoothing for the crossingless unlink. The final stage sends this labeled smoothing to 1, so collectively, $\mathcal{CKh}(\text{Wh}(\Sigma_1))(\Phi) = 1$.

Now consider $\text{Wh}(\Sigma_0)$ and, in particular, the local behavior near a big crossing for $\text{Wh}(\Sigma_1)$, as illustrated in Figure 13. The highlighted band move can be realized as the composition of a Reidemeister II move and a saddle. The induced map on the labeled smoothing for a big crossing leads to merge maps between distinct x -labeled components, from which it follows that $\mathcal{CKh}(\text{Wh}(\Sigma_0))(\Phi) = 0$. \square

Remark 3.4. Note that the process for choosing Φ depended entirely on the decomposition of $\text{Wh}(K)$ into tangles that reflect the overall surface $\text{Wh}(\Sigma_1)$. An entirely identical argument can be used to produce a cycle Φ' that reflects $\text{Wh}(\Sigma_0)$, reversing the roles of the induced maps in the calculations. In particular, we note both maps induced by $\text{Wh}(\Sigma_0)$ and $\text{Wh}(\Sigma_1)$ are nontrivial.

Remark 3.5. Although the surfaces $\text{Wh}(\Sigma_0)$ and $\text{Wh}(\Sigma_1)$ are not minimal genus in B^4 , they are not destabilizable. This is because any surface that is a connected sum with a standard T^2 will induce the trivial map on Khovanov homology with \mathbb{Z}_2 coefficients (or more generally for \mathbb{Z} coefficients, will have image inside $2\mathbb{Z} \subset \mathbb{Z}$), whereas the maps induced by these surfaces are both nontrivial (c.f. 3.3 and 3.4).

Remark 3.6. Non-orientable and higher-genus examples can be obtained by slight modifications to our base example. Replace the clasp on K (from Whitehead doubling a trefoil) with an $-n + \frac{1}{-m}$ rational tangle, illustrated in Figure 14, and produce surfaces analogous to Σ_0 and Σ_1 . Note that $m = n = 1$ corresponds to K . Increasing n increases

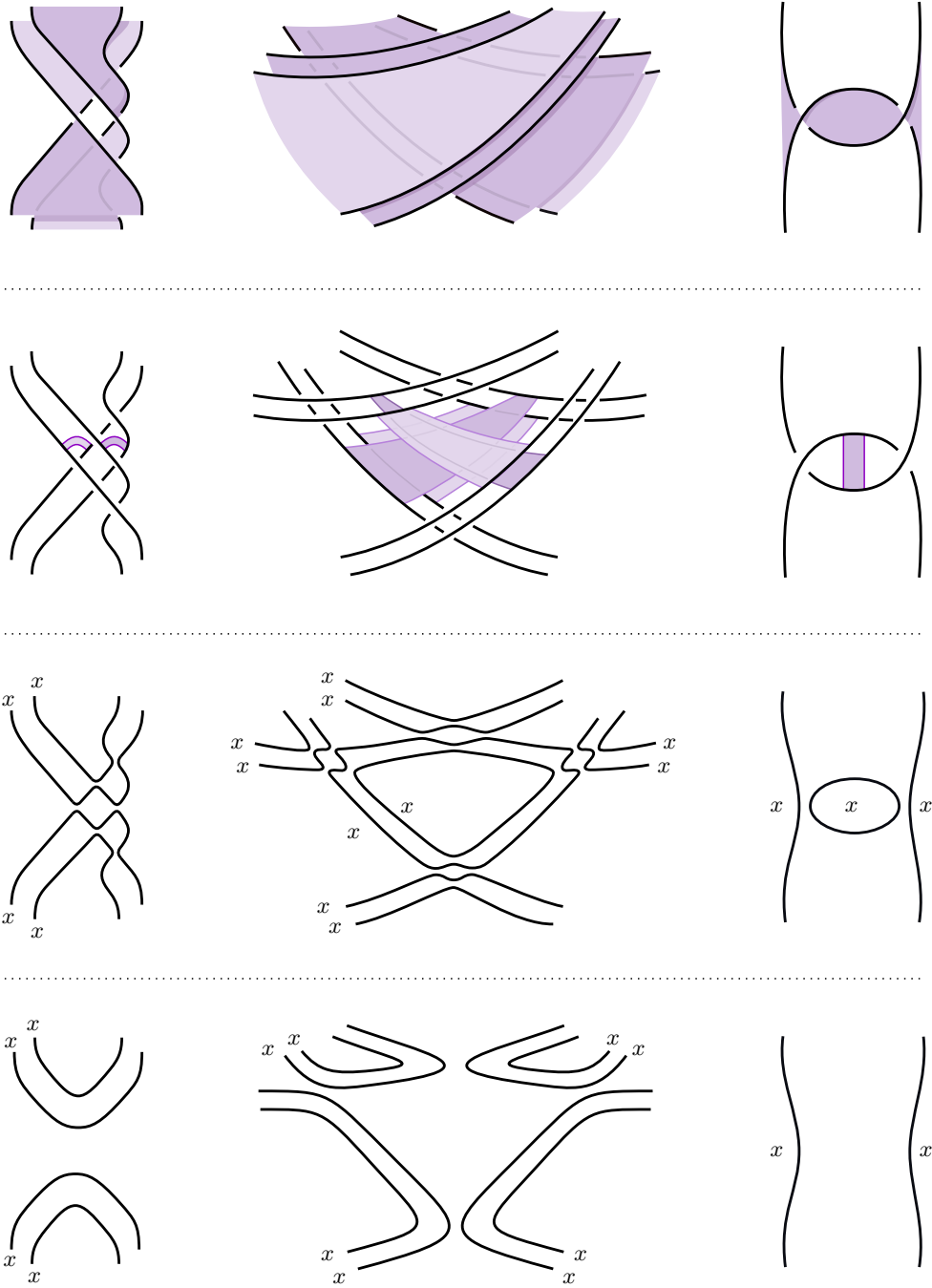


FIGURE 12. By row, top: local pictures of $\text{Wh}(\Sigma_1)$; boundary tangles with bands reflecting the surface they bound; a chosen labeled smoothing for each tangle; the result of applying the maps induced by the band moves (and a sequence of Reidemeister moves) to each labeled smoothing.

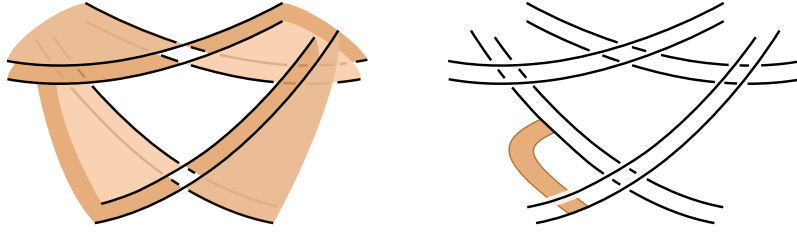


FIGURE 13. A local picture of $\text{Wh}(\Sigma_0)$ near a big crossing for $\text{Wh}(\Sigma_1)$, together with a band used to calculate $\mathcal{CKh}(\text{Wh}(\Sigma_0))$.

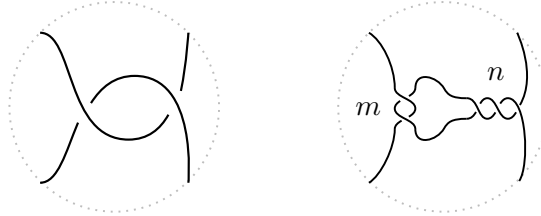


FIGURE 14. Replacing the clasp from K (left) with an $-n + \frac{1}{-m}$ rational tangle (right) produces an infinite family of knots bounding distinct Seifert surfaces for each positive (non-)orientable genus. (Note that m, n denote numbers of half-twists rather than full twists.)

the genus of the surface; increasing m gives an infinite family for each genus (both orientable and non-orientable). As these modifications consist entirely of left-handed crossings, the above arguments persist, so Theorems 1.1 and 1.2 hold for non-orientable, higher-genus surfaces in the smooth rel. boundary setting.

Remark 3.7. The techniques we used to prove Theorem 3.3 appear robust enough to generalize to calculations on larger families of Seifert surfaces. In particular, we expect that whenever a pair of Seifert surfaces for a strongly quasipositive knot J induce distinct maps on Khovanov homology, then so will their positive Whitehead doubles. Moreover, the distinction of their induced maps will be captured by a readily available cycle from $\mathcal{CKh}(\text{Wh}(J))$, produced in a similar manner to Theorem 3.3.

Corollary 3.8. *The surfaces $\text{Wh}(\Sigma_0)$ and $\text{Wh}(\Sigma_1)$ are not related by any diffeomorphism of B^4 (and in particular are not ambiently smoothly isotopic).*

Proof. Suppose there exists a diffeomorphism $f: (B^4, \text{Wh}(\Sigma_0)) \rightarrow (B^4, \text{Wh}(\Sigma_1))$. By Proposition 2.9, the diffeomorphism $f^{-1}|_{S^3}: (S^3, \text{Wh}(K)) \rightarrow (S^3, \text{Wh}(K))$ extends to a diffeomorphism $g: (B^4, \text{Wh}(\Sigma_1)) \rightarrow (B^4, \text{Wh}(\Sigma_1))$. The composition $g \circ f: (B^4, \text{Wh}(\Sigma_0)) \rightarrow (B^4, \text{Wh}(\Sigma_1))$ is the identity on S^3 , contradicting Theorem 3.3. \square

3.4. Whitehead doubles of strongly quasipositive knots. In [Rud90], Rudolph introduced the class of *strongly quasipositive* knots. Though originally defined braid-theoretically, it is convenient (and equivalent) to define such knots as the boundaries of *strongly quasipositive Seifert surfaces*, which are formed from a stack of parallel disks

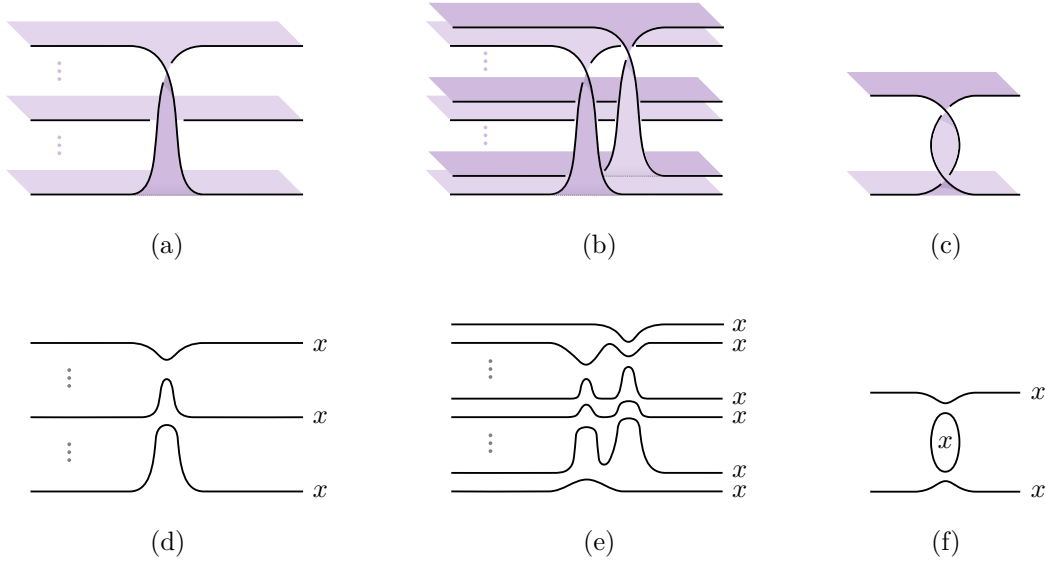


FIGURE 15. (a) A half-twisted band in a strongly quasipositive Seifert surface. (b) Whitehead doubling near a half-twisted band. (c) A fully twisted band forming the clasp in the Whitehead double. (d-e) Labeled smoothings of these regions.

that are joined by embedded, positively half-twisted bands as in Figure 15(a). (These disks and bands are oriented so that the surface's boundary is naturally braided.)

Proposition 3.9. *If S is a strongly quasipositive Seifert surface for a knot J , then $\text{Wh}(S)$ induces a nontrivial map from $\text{Kh}(\text{Wh}(J))$ to \mathbb{Z}_2 .*

Proof. Given S formed from n disks joined by ℓ bands as in Figure 15(a), we first form the normal pushoff of S by introducing an additional n disks and ℓ bands as in Figure 15(b). We give this pushoff the opposite orientation as that of S . To complete $\text{Wh}(S)$, we add one more band between the top two sheets as in Figure 15(c).

We consider an element in $\text{Kh}(\text{Wh}(J))$ that is essentially the Whitehead double of Plamenevskaya's invariant $\psi(J)$ (when J is viewed as an n -stranded braid) [Pla06]. Recall that Plamenevskaya's chain element is given by the smoothing of the n -braid J as n concentric circles as in Figure 15(d), with all circles labeled with an x . Consider the similarly constructed element of $\text{CKh}(\text{Wh}(J))$, where the regions from parts (b) and (c) of Figure 15 are smoothed and labeled as in parts (e) and (f). All 0-resolved crossings join distinct x -labeled circles, so this chain element is a cycle. A calculation entirely analogous to the one given in Figure 12 shows that $\text{Kh}(\text{Wh}(S))$ maps the described element of $\text{Kh}(\text{Wh}(J))$ to 1 in $\mathbb{Z}_2 = \text{Kh}(\emptyset)$, as desired. \square

We may now prove Theorem 1.6, which we restate slightly more precisely.

Theorem 3.10. *If J is a nontrivial strongly quasipositive knot of Seifert genus g , then $\text{Wh}(J)$ bounds at least two Seifert surfaces of genus $2g$ that are topologically isotopic rel. boundary in B^4 yet are not related by any diffeomorphism of B^4 (and in particular are not ambiently smoothly isotopic).*

Proof. Let S be a strongly quasipositive Seifert surface for J , which has genus $g \geq 1$ because J is not the unknot. Let $\text{Wh}(S)$ denote its Whitehead double, which has genus $g(\text{Wh}(S)) = 2g \geq 2$. By the proposition above, $\text{Wh}(S)$ induces a nontrivial map on Khovanov homology with \mathbb{Z}_2 -coefficients.

On the other hand, consider the genus-2 g Seifert surface for $\text{Wh}(J)$ obtained from the standard genus-1 Seifert surface for $\text{Wh}(J)$ by stabilizing $2g - 1$ times. Any stabilized surface induces a trivial map on Khovanov homology with \mathbb{Z}_2 -coefficients. Since the Whitehead doubled surface $\text{Wh}(S)$ induces a nontrivial map, it cannot be destabilized, hence there can be no diffeomorphism of B^4 carrying $\text{Wh}(S)$ to the stabilized surface.

On the other hand, these genus-2 g Seifert surfaces are topologically isotopic rel. boundary in B^4 by Theorem 2.7. \square

3.5. Minimal genus examples and discussion. We now modify our previous examples to obtain the minimal genus examples claimed in Theorem 1.2. Note that the (untwisted) Whitehead double of any knot bounds a standard genus-1 Seifert surface, so the Seifert surfaces constructed in Section 2.4 will never minimize the Seifert genus of their boundary (see Proposition 2.5).

To this end, we consider a knot K_T obtained as a band sum of $\text{Wh}(K)$ with the right-handed trefoil as shown in Figure 16. Note that we have not specified how many full twists are in the band, so K_T actually refers to any member of an infinite family of knots. These knots can be distinguished by their Khovanov homologies [Wan22] or by their hyperbolic volumes; see the ancillary files [HKM⁺].

Because the band has been chosen to avoid both $\text{Wh}(\Sigma_0)$ and $\text{Wh}(\Sigma_1)$, we can sum these surfaces with the standard Seifert surface for the trefoil T to produce two genus-3 Seifert surfaces Σ_0^T and Σ_1^T for K_T . On the other hand, the band intersects the standard genus-1 Seifert surface for $\text{Wh}(K)$ in an essential way, leading to an increase in the Seifert genus. Moreover, this eliminates all symmetries of the knot, which allows us to avoid an analysis like the one given in Proposition 2.9.

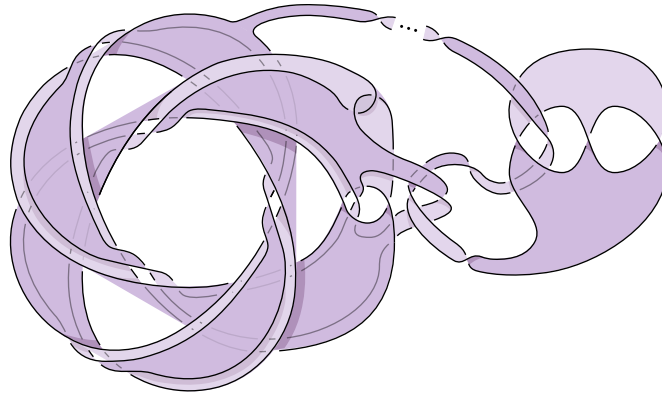


FIGURE 16. The Seifert surface Σ_1^T obtained by band summing $\text{Wh}(\Sigma_1)$ and a fiber for the trefoil (where the ellipsis indicates any number of full twists). The boundary of the surface is the knot K_T .

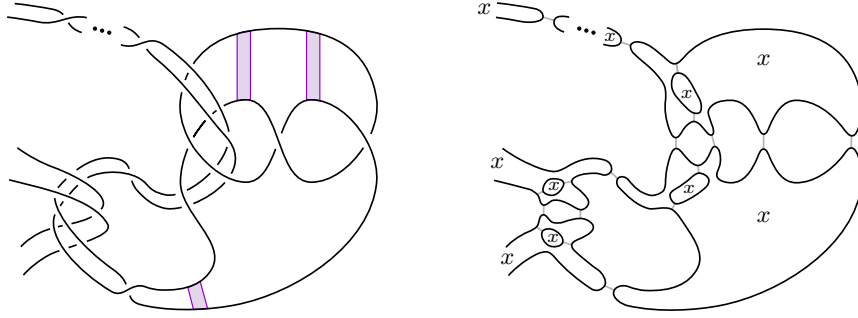


FIGURE 17. Left: bands giving a movie of Σ_1^T near T . Right: a labeled smoothing of the corresponding tangle near T

Proposition 3.11. *The knot K_T has Seifert genus 3 and trivial symmetry group.*

Proof. The Seifert genus of K_T can be computed with the HFKCalculator [Sza19]; the symmetry group of $S^3 \setminus K_T$ (along with hyperbolicity of this complement) can be checked in SnapPy [CDGW] inside Sage [The19]. We refer the reader to the ancillary files of this paper [HKM⁺] for documentation. \square

Proof of Theorem 1.2. By Proposition 3.11, we have that Σ_0^T and Σ_1^T are minimal genus Seifert surfaces. Since $\text{Wh}(\Sigma_0)$ and $\text{Wh}(\Sigma_1)$ are topologically isotopic rel. boundary when pushed into B^4 , so are Σ_0^T and Σ_1^T .

The band moves shown on the left side of Figure 17 determine a link cobordism S from K_T to $\text{Wh}(K)$, and we may view the surfaces Σ_0^T and Σ_1^T as compositions $\text{Wh}(\Sigma_0) \circ S$ and $\text{Wh}(\Sigma_1) \circ S$. Next, let $\Psi \in \text{CKh}(K_T)$ be the labeled smoothing that extends $\Phi \in \text{CKh}(\text{Wh}(K))$ using the right half of Figure 17. It is straightforward to check that Ψ is a cycle and that the map $\text{CKh}(S)$ sends Ψ to Φ . It follows that $\text{CKh}(\Sigma_0^T)(\Psi) = \text{CKh}(\text{Wh}(\Sigma_0))(\Phi) = 0$ and $\text{CKh}(\Sigma_1^T)(\Psi) = \text{CKh}(\text{Wh}(\Sigma_1))(\Phi) = 1$. This immediately implies that Σ_0^T and Σ_1^T are not smoothly equivalent rel. boundary. By Proposition 3.11, we know K_T has trivial symmetry group, so we further conclude that there is no diffeomorphism of B^4 taking Σ_0^T to Σ_1^T . \square

Interestingly, it is not clear how to perform analogous computations of knot Floer cobordism maps that obstruct two Seifert surfaces from becoming smoothly isotopic when pushed into B^4 . Consider the following proposition, which follows immediately from functoriality and the grading shift calculations of Juhász–Marengon [JM18].

Proposition 3.12. *If S is a Seifert surface for a knot J in S^3 such that $g(S) > g_3(J)$ and is decorated so that either the z -region or w -region is a bigon, then S induces a trivial map on $\widehat{\text{HFK}}(J)$. Moreover, any Seifert surface for another knot J' into which S embeds also induces a trivial map on $\widehat{\text{HFK}}(J')$.*

In particular, this means that the usual cobordism maps on $\widehat{\text{HFK}}$ with trivial decorations cannot distinguish Seifert surfaces that are not of minimal Seifert genus. In contrast, our examples in Theorem 3.3 are distinctly *not* minimal genus Seifert surfaces. The surfaces in Theorem 1.2 are minimal genus, but contain subsurfaces that are not

minimal genus (specifically, the surfaces from Theorem 3.3). Thus, we cannot *easily* use the knot Floer cobordism maps to distinguish two Seifert surfaces in B^4 . In order to do so, one would either have to work with nontrivial decorations, find some new way of producing minimal genus examples, or perhaps use a further refinement of knot Floer homology (as opposed to \widehat{HFK}).

4. OBSTRUCTIONS FROM BRANCHED COVERS

4.1. A topological counterexample. Let Σ_0 and Σ_1 be the surfaces of Figure 1, with interiors pushed slightly into B^4 .

Theorem 4.1. *Let X_i be the double cover of B^4 branched along Σ_i for $i = 0, 1$. The manifolds X_0 and X_1 are not homeomorphic.*

Theorem 4.1 implies Theorem 1.1, since a locally flat isotopy from Σ_0 to Σ_1 would induce a homeomorphism from X_0 to X_1 .

Proof of Theorem 4.1. In Figure 18, we illustrate simple closed curves a_0, b_0 on Σ_0 and a_1, b_1 on Σ_1 that span the first homology. The resulting Seifert matrices (after appropriately orienting) are

$$V_0 := \begin{pmatrix} -6 & -2 \\ -3 & -2 \end{pmatrix} \text{ for } \Sigma_0 \quad \text{and} \quad V_1 := \begin{pmatrix} -6 & 0 \\ 1 & -1 \end{pmatrix} \text{ for } \Sigma_1.$$

The intersection form of $H_2(X_i; \mathbb{Z})$ is given by $V_i + V_i^T$, where the basis comes from doubling relative homology classes in $B^4 \setminus \nu(\Sigma_i)$ bounded by a_i and b_i [Kau72]. One can see this explicitly in the handle diagrams of X_0 and X_1 in the bottom of Figure 18, obtained via the procedure of [AK80, Section 2]. In particular, X_1 contains a locally flat embedded oriented surface F whose Euler number is -2 . On the other hand, the intersection form on $H_2(X_0; \mathbb{Z})$ is

$$V_0 + V_0^T = \begin{pmatrix} -12 & -5 \\ -5 & -4 \end{pmatrix}.$$

Letting A_0 and B_0 denote the corresponding generators of $H_2(X_0; \mathbb{Z})$, we see that

$$\begin{aligned} (mA_0 + nB_0) \cdot (mA_0 + nB_0) &= -12m^2 - 4n^2 - 10mn \\ &= -2(6m^2 + 2n^2 + 5mn). \end{aligned}$$

If there were a homeomorphism from X_1 to X_0 , then the image of F would have Euler number ± 2 , implying that there is an integer solution to

$$6m^2 + 2n^2 + 5mn = \pm 1.$$

Solving for n , the discriminant of this equation is

$$(5m)^2 - 4 \cdot 2 \cdot (6m^2 \mp 1) = -23m^2 \pm 8.$$

We must have this term be nonnegative to have a real solution. Since m is an integer, we obtain $m = 0$. This yields $2n^2 = \pm 1$, a contradiction. \square

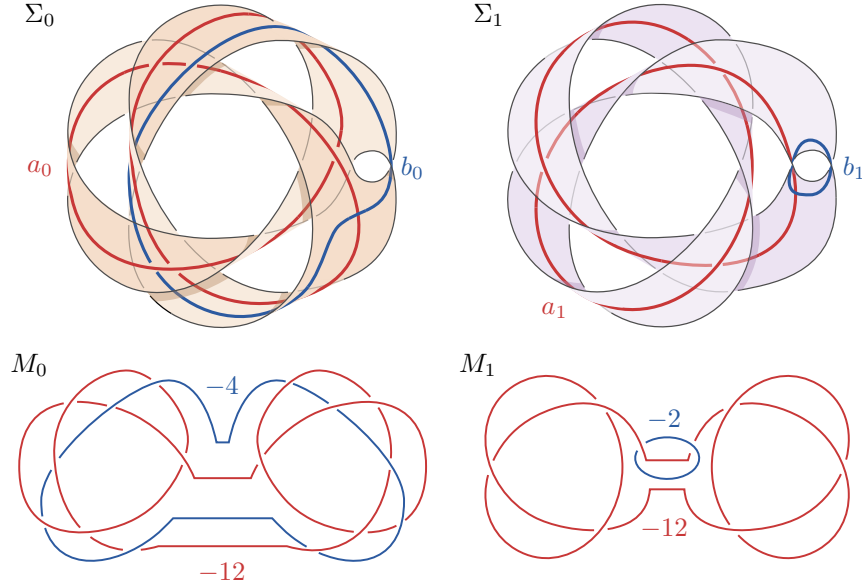


FIGURE 18. Top: a symplectic basis on each of Σ_0 and Σ_1 . Bottom: handle diagrams for the double branched covers X_0 and X_1 .

Remark 4.2. We find the argument of Theorem 4.1 striking in that its methods are extremely elementary and have been known to topologists for fifty years, yet are sufficient to answer a question in the literature that has been open for forty years.

Remark 4.3. As shown in Figure 2, the union of the surfaces Σ_0, Σ_1 in S^3 is a standard genus-2 surface. Thus, even though Σ_0, Σ_1 are not topologically isotopic in B^4 , their union $(B^4, \Sigma_0) \cup \overline{(B^4, \Sigma_1)}$ forms a smoothly unknotted closed surface in S^4 . It seems unlikely that gluing together modifications of the examples in this paper could produce oriented exotically knotted closed surfaces in S^4 .

Remark 4.4. A tube can be added to each of Σ_0 and Σ_1 to obtain a pair of genus-1 surfaces that are isotopic rel boundary in B^4 . (Or in other words, Σ_0 and Σ_1 have *stabilization distance* one.) We illustrate this in Figure 19; here we draw a ribbon surface in B^4 by drawing its boundary knot and bands attached to that knot representing index-1 points of the surface with respect to radial height.

In the top row of Figure 19, we show that two particular bands attached to a link are isotopic. (Note that we allow the ends of the bands to slide along the link, and we allow the two bands to pass through each other). This link is obtained by surgering K along the other three bands in the bottom two illustrations. We conclude that the surfaces illustrated in the bottom of Figure 19 are smoothly isotopic rel. boundary in B^4 . The surface on the left is obtained from Σ_0 by attaching a single tube and the surface on the right is obtained from Σ_1 by attaching a single tube.

Remark 4.5. We can modify Σ_0 and Σ_1 to produce pairs of non-orientable surfaces; see Remark 3.6 or simply consider the specific pair Σ'_0 and Σ'_1 in Figure 20. The 2-fold

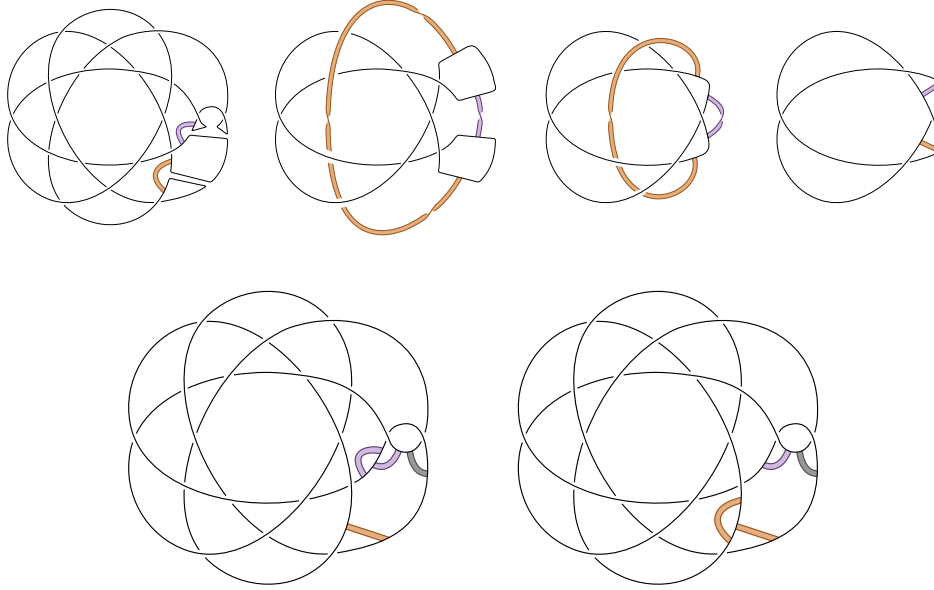


FIGURE 19. Top row, from left to right: We draw two bands attached to a link. We produce an isotopy from one band to the other. Bottom row: We conclude that the two indicated surfaces are smoothly isotopic rel. boundary in B^4 .

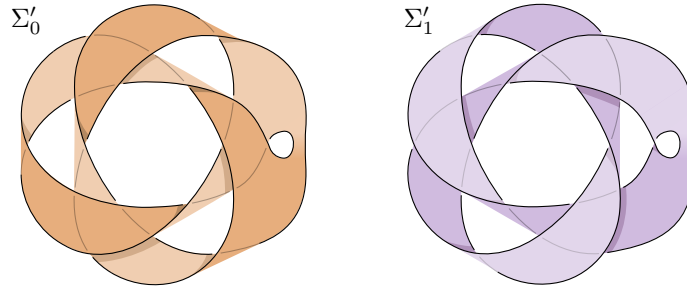


FIGURE 20. Non-orientable surfaces that are not topologically isotopic in B^4 .

branched covers X'_0, X'_1 of B^4 branched along Σ'_0, Σ'_1 (after pushing their interiors into the interior of B^4) have intersection forms on H_2 respectively presented by

$$\begin{pmatrix} -12 & -5 \\ -5 & -3 \end{pmatrix} \quad \text{and} \quad \begin{pmatrix} -12 & 1 \\ 1 & -1 \end{pmatrix},$$

which can be easily distinguished by e.g. the same argument as in Theorem 4.1 (there is no embedded, oriented locally flat surface in X'_0 with Euler number -1 , while there is in X'_1). Therefore, the surfaces Σ'_0 and Σ'_1 are not topologically isotopic in B^4 .

As an aside, we note that the intersection form argument of Theorem 4.1 can imply other interesting results about the structure of a surface in B^4 . For example, consider the Möbius band M bounded by the knot 8_{20} illustrated in Figure 21 (left). The double cover X of B^4 branched along M admits a handle decomposition consisting of

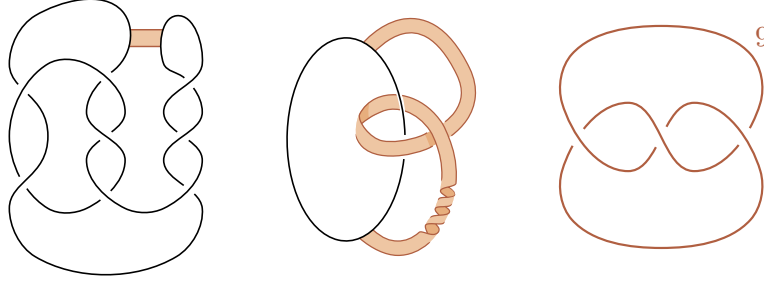


FIGURE 21. Left: A Möbius band M in B^4 bounded by 8_{20} , consisting of a disk bounded by the drawn curve together with the indicated nonorientable band. Middle: we isotope the left picture. Right: we obtain the double cover of B^4 branched along M via the procedure of [AK80] (see also [GS99, Section 6.3] or [Akb16, Chapter 11]).

a 0-handle and a 2-handle attached along a right-handed trefoil with framing 9. We conclude from the intersection form on $H_2(X; \mathbb{Z})$ that X does not admit a \mathbb{CP}^2 or $\overline{\mathbb{CP}}^2$ summand, and hence M does not decompose topologically as a connected sum of an unknotted projective plane and a slice disk for 8_{20} . Of course, this would be obvious in the case that ∂M were not slice – but given that 8_{20} is slice, this is not so clear and might be viewed as a negative answer to a relative version of the Kinoshita conjecture, which asks whether every projective plane in S^4 decomposes as a connected sum of a knotted 2-sphere and an unknotted projective plane.

Corollary 4.6. *Any 1-minimum ribbon Möbius band M properly embedded in B^4 whose boundary is a knot J with $\det(J) > 1$ does not decompose topologically as a connected sum of a slice disk for J and an unknotted projective plane.*

Corollary 4.6 applies to the Möbius band for $8_{20} = P(2, -3, 3)$ featured in Figure 21, as well as the analogous Möbius band for the slice pretzel knot $P(2n, -2n - 1, 2n + 1)$ for any $n \geq 1$. (Note that this knot has determinant $4n^2 + 4n + 1$.) Each of these pretzel knots admits a standard ribbon disk obtained by a band move across the even strand. It is a relatively easy exercise to check that gluing this disk to the described Möbius band yields a smoothly unknotted projective plane in S^4 .

Proof of Corollary 4.6. Since M has one minimum, one saddle, and no maxima, the 2-fold cover X of B^4 branched along M can be built from a single 0-handle and 2-handle. The boundary of X is the 2-fold cover of S^3 branched over J , which has first homology of order $\det(J)$. This must then be the framing of the 2-handle up to sign, so the intersection form on $H_2(X; \mathbb{Z}) = \mathbb{Z}$ is $[\pm \det(J)]$. We conclude that X does not admit a \mathbb{CP}^2 or $\overline{\mathbb{CP}}^2$ summand and hence M does not admit an unknotted projective plane summand. \square

4.2. Infinite families of surfaces up to isotopy rel boundary. In this section, we prove Theorems 1.4 and 1.5 by constructing two infinite families of surfaces that are not isotopic rel. boundary. In the first case, the surfaces are disconnected but not even

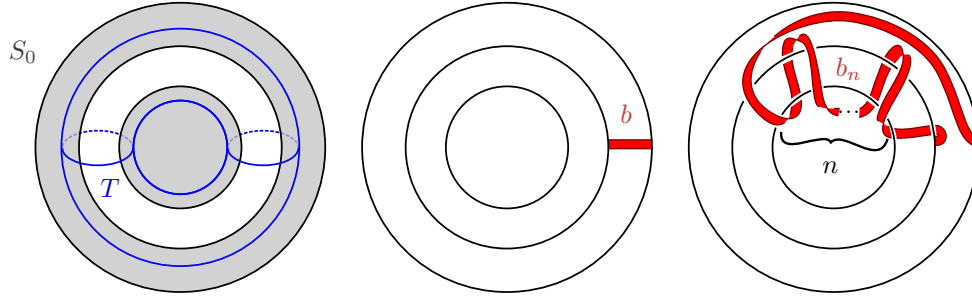


FIGURE 22. Left: the surface S_0 and the torus T . Middle: the band b . Right: the band b_n .

topologically isotopic rel. boundary, while in the second case the surfaces are connected but we give only a smooth obstruction to isotopy rel. boundary.

We begin with Theorem 1.5. Consider the surface S_0 in Figure 22. This surface is a split union of a disk and an annulus; we illustrate a torus T intersecting S_0 in two circles. Let S_n be obtained from S_0 by performing n meridional twists to S_0 about T .

Proposition 4.7. *For $n \neq 0$, the surfaces S_n and S_0 are not topologically isotopic rel. boundary.*

Proof. First note that S_n is freely isotopic S_0 . Indeed, S_n is obtained from S_0 by applying n meridional twists τ along the torus T in the complement of the unlink ∂S_0 . As mentioned in §2.3, the diffeomorphism τ of S^3 (which is supported near T) is isotopic to the identity via an isotopy supported near the solid torus that T bounds in Figure 22 (left). Push the interiors of S_0 and S_n into B^4 , and extend τ over B^4 to preserve the relation $S_n = \tau^n(S_0)$.

Towards a contradiction, suppose S_n is isotopic to S_0 rel. boundary in B^4 . Consider the enlarged surfaces $S_0^b, S_n^b \subset B^4$ obtained by attaching the band $b \subset S^3$ shown in Figure 22 to each of $S_0, S_n \subset B^4$, respectively. Note that the isotopy rel. boundary between S_0 and S_n induces an isotopy between S_0^b and S_n^b . Rather than study S_n^b directly, it will be simpler to consider its pullback $F_n = \tau^{-n}(S_n^b)$ which, by construction, is isotopic to S_0^b . Observe that

$$F_n = \tau^{-n}(S_n \cup b) = \tau^{-n}(S_n) \cup \tau^{-n}(b) = S_0 \cup \tau^{-n}(b),$$

so F_n is equivalently obtained from S_0 by attaching the band $b_n = \tau^{-n}(b)$ from Figure 22 (right). In Figure 23, we redraw S_0^b and F_n and produce Kirby diagrams of the 2-fold branched covers of B^4 over S_0^b and F_n . We see that

$$H_1(\Sigma(S_0^b); \mathbb{Z}) = \mathbb{Z} \quad \text{while} \quad H_1(\Sigma(F_n); \mathbb{Z}) = \mathbb{Z}_{2|n|}.$$

This contradicts F_n being freely isotopic to S_0^b , hence S_0 and S_n cannot be isotopic rel. boundary in B^4 . \square

The next corollary implies Theorem 1.5.

Corollary 4.8. *For $m \neq n$, the surfaces S_m and S_n are not topologically isotopic rel. boundary.*

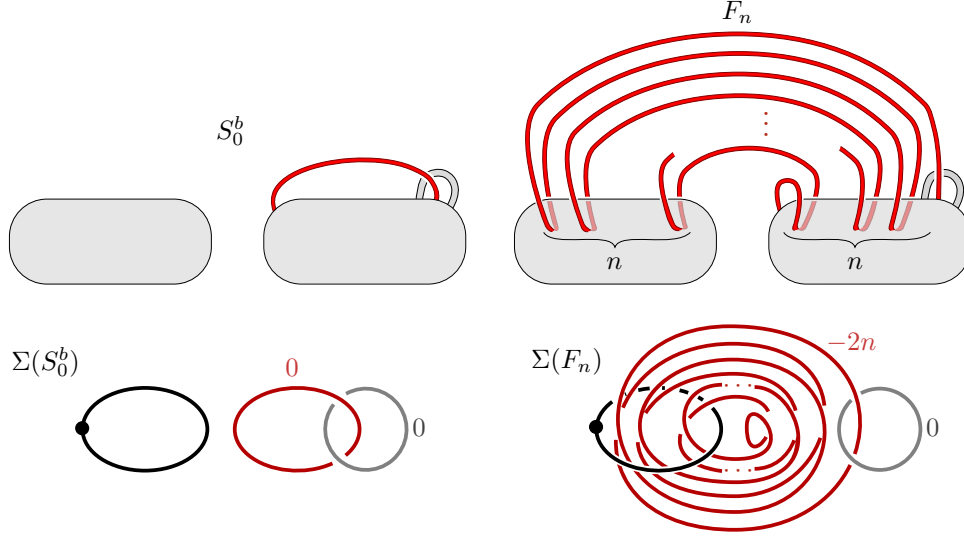


FIGURE 23. In the top row, we draw S_0^b and F_n as ribbon surfaces in B^4 . If S_0 and S_n are isotopic rel. boundary, then S_0^b and F_n are freely isotopic. In the bottom row, we perform the algorithm of [AK80] to obtain Kirby diagrams of the respective 2-fold branched covers $\Sigma(S_0^b)$ and $\Sigma(F_n)$.

Proof. There is a homeomorphism of B^4 that maps S_m and S_n to S_0 and S_{n-m} , respectively. Since S_0 and S_{n-m} are not topologically isotopic rel. boundary, neither are S_m and S_n . \square

We now proceed to the proof of Theorem 1.4. The construction similarly relies on torus twisting, but we can arrange for the surfaces in question to be connected at the cost of complicating the boundary link. To that end, let $S = S_0$ be the surface in Figure 24, which is isotopic to the surface S_0 from Example 2.3 (originally shown in the center of Figure 5). Example 2.3 also introduced surfaces S_n obtained from S_0 by twisting n times about the torus T pictured in Figure 5 (right). Our first step in distinguishing these Seifert surfaces up to smooth isotopy rel. boundary in B^4 will be to show that the double branched cover $M_n = \Sigma_2(B^4, S_n)$ is obtained from $M = \Sigma_2(B^4, S)$ by surgery along the torus T' depicted in Figure 24 (right).

Proposition 4.9. *The 4-manifold M shown in the left of Figure 25 is the double branched cover of B^4 along $S = S_0$.*

Proof. In Figure 24 we obtain a Kirby diagram for the double branched cover of B^4 along S , using the algorithm of [AK80]. In Figure 26, we show how to perform Kirby moves to this diagram to arrive at Figure 25 (left). \square

Following the above Kirby moves also shows that the torus T' depicted in Figure 24 is isotopic to the obvious torus $T^2 \times 0$ in the copy of $T^2 \times D^2 \subset M$ depicted in Figure 25. The second manifold $M_{(0,1,0)}$ in Figure 24 is obtained by surgery on this torus T' , and the surgery is of type $(0, 1, 0)$ relative to the basis shown.

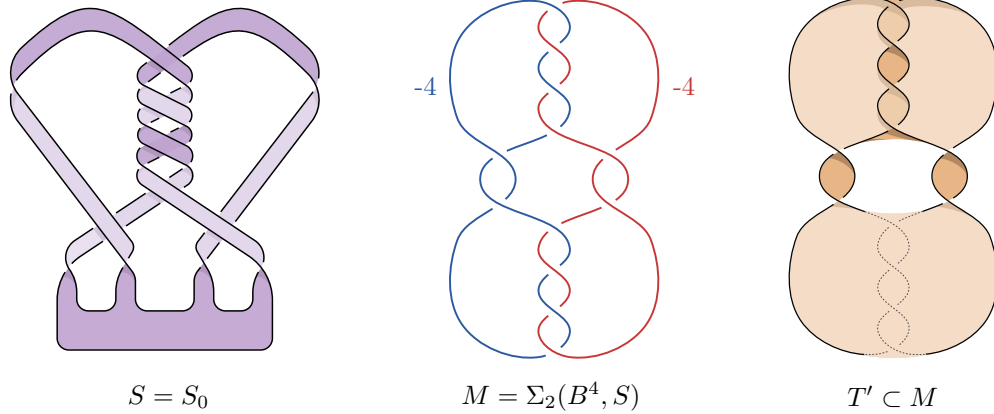


FIGURE 24. Left: An alternative diagram for the surface from Example 2.3. Center: A Kirby diagram for the 2-fold branched cover of B^4 along S . Right: A torus T' of square zero, consisting of a genus-1 surface in S^3 and the core disks of the two 2-handles in the middle diagram. In Proposition 4.10, we show that the lift of T in $S^3 \setminus L$ consists of two parallel copies of T' .

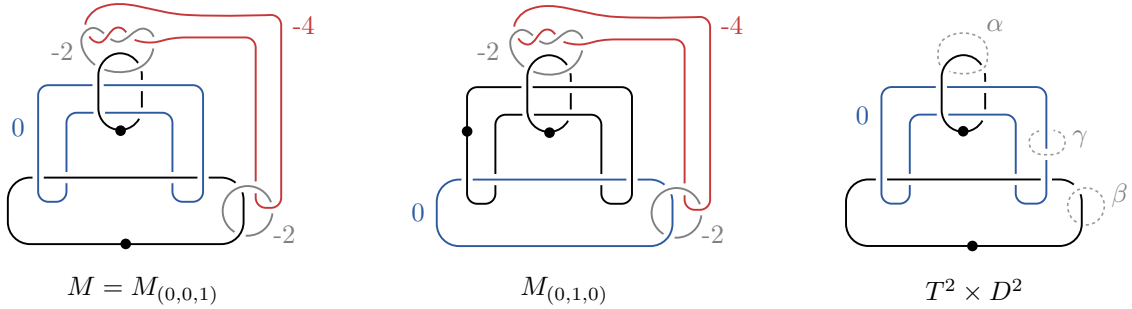


FIGURE 25. Left: a 4-manifold M . Right: A copy of $T^2 \times D^2$ contained in M , with curves α, β, γ in $\partial T^2 \times D^2$ indicated. The torus $T^2 \times 1$ is equivalent T' from Figure 24. Here, $\gamma = \text{pt} \times \partial D^2$, so surgering M along $T^2 \times 0$ gluing a meridian disk to $(0, 0, 1)$ in (α, β, γ) coordinates is the trivial surgery (and hence M can be identified with $M_{(0,0,1)}$). Middle: A diagram of $M_{(0,1,0)}$.

Proposition 4.10. *The torus $T \subset S^3 \setminus L$ of Figure 5 lifts to two copies of obvious torus T' inside M (after being pushed into the interior of M).*

Proof. In S^3 , the torus T bounds a solid torus V intersecting L in two circles that are both cores of the solid torus. Then V lifts to a copy of $T^2 \times I$ in ∂M , so we conclude that the lift of T to M consists of two disjoint, parallel tori in ∂M .

To identify these tori upstairs, one could perform this lift explicitly and obtain parallel copies of the torus illustrated in the right of Figure 24, which is the torus visible in Figure 25. Instead, we will appeal to an indirect argument, as follows.

In the diagram of M given in Figure 24, the branched covering involution of ∂M (whose quotient is S^3) corresponds to rotation about a horizontal axis. By considering

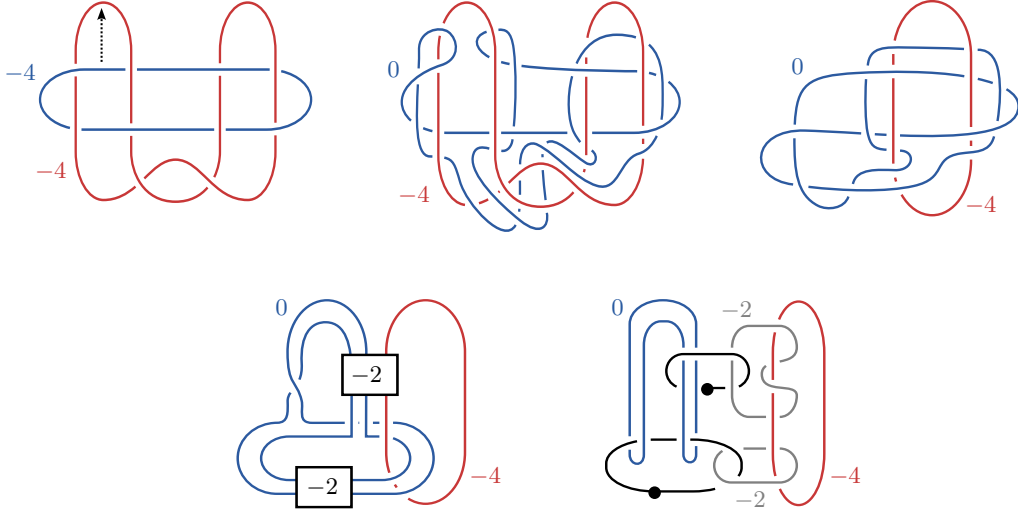


FIGURE 26. Beginning with the diagram of M on the top left (obtained from Figure 24 by isotopy), we perform Kirby moves until arriving at the alternative diagram of M on the bottom right, which is isotopic to the diagram of M in Figure 25.

the diagram of T' in Figure 24 (right), we see that positive and negative pushoffs of T' can be taken disjoint from the branch set and are exchanged by the covering involution. We conclude that they project to a single embedded torus \hat{T} in $S^3 \setminus L$. Since T' is nonseparating in ∂M , there must be components of L on each side of \hat{T} , and \hat{T} cannot be boundary-parallel in $S^3 \setminus \nu(L)$. Since L is non-split, then \hat{T} is essential.

From Figure 5, it is straightforward to see that $S^3 \setminus L$ contains exactly two essential tori that are not boundary parallel (up to isotopy). One is the torus T that encloses two components of L , and the second torus encloses a single component of L which sits as a twisted Whitehead pattern knot inside in enclosed solid torus. The double branched cover of the solid torus over the Whitehead pattern knot is not $T^2 \times I$, so this second torus in $S^3 \setminus L$ does not lift to parallel copies of T' . We conclude that \hat{T} is isotopic to T , as claimed. \square

Proposition 4.11. *The double branched cover M_n of B^4 along S_n is the 4-manifold $M_{(0,2n,1)}$ obtained from M by $(0, 2n, 1)$ -surgery along T' .*

Proof. Recall that S_n is obtained from S_0 by twisting n times about T . By Proposition 4.10, the lift of T to M consists of two parallel copies of T' . Then M_n is obtained from M by performing degree-1 surgeries on each of two parallel copies of T' in the direction of the twist. In our chosen coordinates, the direction is $n\beta$, so M_n is obtained from M by performing $(0, n, 1)$ surgeries along two copies of T' .

Finally, in Figure 27, we adapt the construction from [Akb13] to show that performing $(0, n, 1)$ -surgeries on two parallel copies of T' yields the same manifold up to diffeomorphism rel. boundary as performing one $(0, 2n, 1)$ -surgery along T' . \square

With this topological setup in place, we now distinguish the surfaces' branched covers.

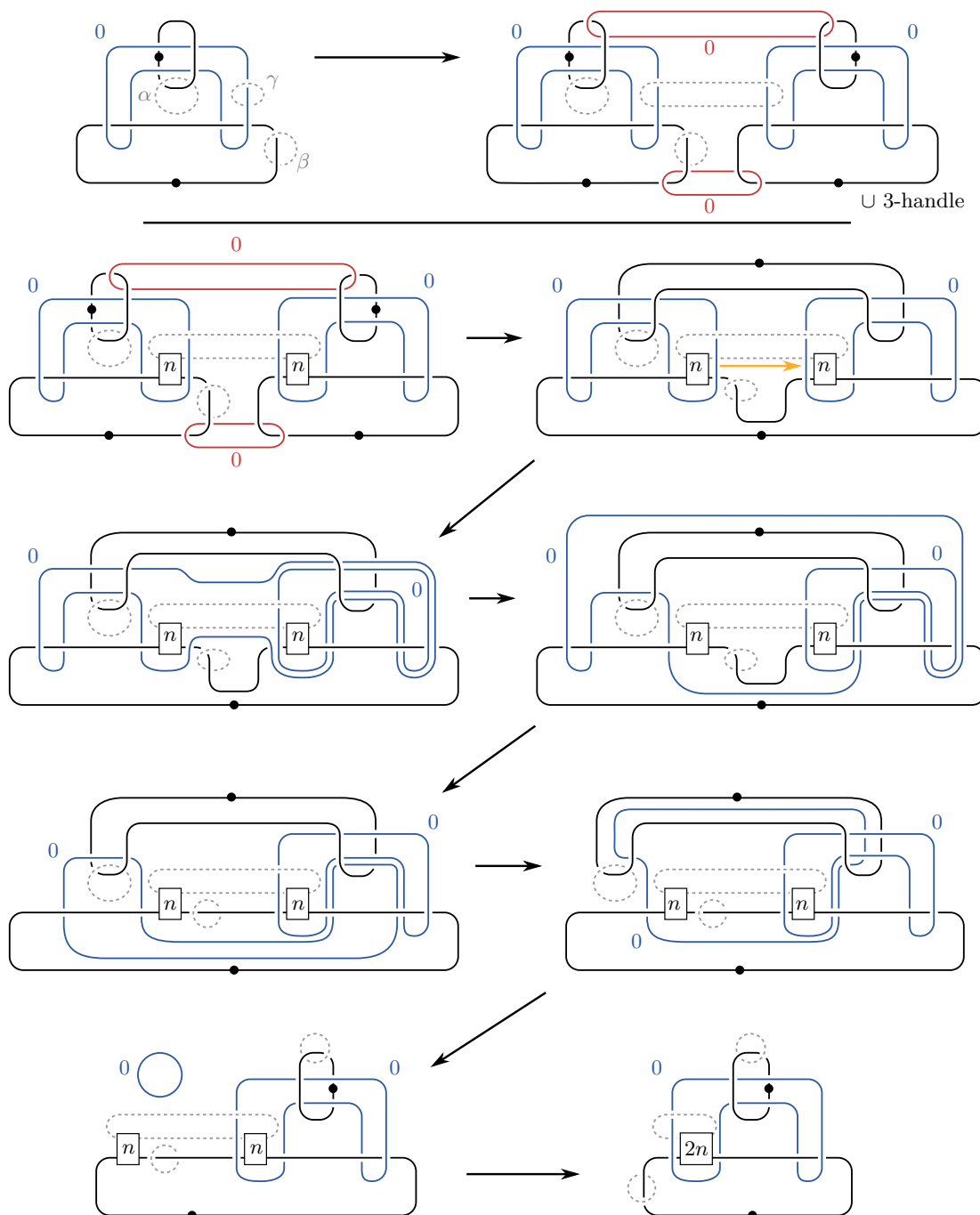


FIGURE 27. Top left: a diagram of $T^2 \times D^2$. Top right: we perform Kirby moves so as to make two copies of $T^2 \times \{\text{pt}\}$ easily visible. Second row and down, following arrows: we perform $(0, n, 1)$ surgery on two parallel copies of $T^2 \times \{\text{pt}\}$ and then perform Kirby moves to show that the result is diffeomorphic to the result of performing $(0, 2n, 1)$ surgery along $T^2 \times 0$. We note that the final step consists of a 2-/3-handle cancellation.

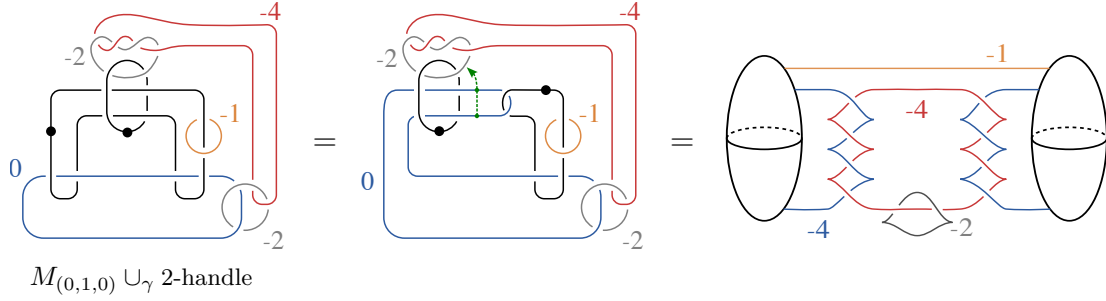


FIGURE 28. On the left, a handle diagram for the 4-manifold obtained by attaching a (-1) -framed 2-handle to $\gamma \subset \partial M_{(0,1,0)}$. The second diagram is obtained by isotopy. After performing the two handleslides indicated in the second diagram and canceling a $1/2$ -handle pair, we obtain the (Stein) handle diagram on the right.

Proposition 4.12. *The 4-manifolds $M_{(0,2n,1)}$ are all distinct up to diffeomorphism rel. boundary.*

Proof. We will construct a 4-dimensional cap Q with $\partial Q = -\partial M$ and distinguish the closed 4-manifolds $Z_n = M_{(0,2n,1)} \cup Q$. To construct the cap, we begin by viewing ∂M as $\partial M_{(0,1,0)}$ (Figure 25, middle). Attach a (-1) -framed 2-handle to $M_{(0,1,0)}$ along γ . As demonstrated in Figure 28, the resulting 4-manifold admits the structure of a Stein domain [Gom98]. By work of Lisca-Matić [LM97], it embeds into a closed, minimal Kähler surface Z that can be chosen to satisfy $b_2^+ > 1$ and $K_Z \cdot K_Z > 0$ for the canonical class $K_Z = -c_1(Z) \in H^2(Z; \mathbb{Z})$. Let Q be the 4-manifold $Z \setminus \mathring{M}_{(0,1,0)}$.

Let Z_0 denote the 4-manifold $M \cup Q$, and extend this to an infinite family $Z_n = M_{(0,2n,1)} \cup Q$. By construction, Z_n is obtained from Z_0 by torus surgery of type $(0, 2n, 1)$, and Z is obtained from Z_0 by surgery of type $(0, 1, 0)$. It follows from the Morgan-Mrowka-Szabó formula [MMS97, Theorem 1.1] that the Seiberg-Witten invariants of Z_n can be computed in terms of the invariants of Z , the $(0, 1, 0)$ -surgery, and Z_0 , the $(0, 0, 1)$ -surgery.

We collect some observations that simplify this calculation. First, we claim that Z_0 has vanishing Seiberg-Witten invariants. Recall that the construction of Q involved attaching a (-1) -framed 2-handle to ∂M along the curve γ . Since γ bounds a smoothly embedded disk in M , it follows that $Z_0 = M \cup Q$ contains a smoothly embedded 2-sphere of square -1 . Moreover, since γ is a meridian to the 0-framed 2-handle in M , this 2-sphere intersects the surgery torus $T^2 \times \{0\} \subset M$ transversely in a single point. It follows that the sum of these homology classes can be represented by a torus of square $+1$. This violates the adjunction inequality, so there cannot exist any Seiberg-Witten basic classes on Z_0 . Turning to the Kähler surface Z , note that the only Seiberg-Witten basic classes are $\pm K_Z$ and that $|\text{SW}_Z(K_Z)| = 1$ [Mor96].

To calculate the invariants of Z_n , let $\kappa \in H_2(Z; \mathbb{Z})$ denote the Poincaré dual of K_Z , and let κ_n denote any class in $H_2(Z_n; \mathbb{Z})$ such that the Spin^c structures on Z_n and Z corresponding to κ_n and κ , respectively, coincide where these 4-manifolds agree (i.e., away from the torus surgery neighborhood $T^2 \times D^2$). Let us also use $[T]$ in each of

$H_2(Z_n; \mathbb{Z})$ and $H_2(Z; \mathbb{Z})$ to denote the dual torus *after* surgery (i.e., the class of the core torus $T^2 \times \{0\}$ after regluing $T^2 \times D^2$ to perform the torus surgery). With this notation in place, the preceding observations combine with [MMS97, Theorem 1.1] to imply that the only Seiberg-Witten basic classes on Z_n are those of the form $\pm\kappa_n + i[T]$ for $i \in \mathbb{Z}$, and that the sums of the Seiberg-Witten invariants of these classes satisfy

$$\begin{aligned} \sum_{i \in \mathbb{Z}} \text{SW}_{Z_n}(\kappa_n + i[T]) &= 2n \sum_{i \in \mathbb{Z}} \text{SW}_Z(\kappa + i[T]) = 2n(\text{SW}_Z(\kappa) + 0) = \pm 2n \\ \sum_{i \in \mathbb{Z}} \text{SW}_{Z_n}(-\kappa_n + i[T]) &= 2n \sum_{i \in \mathbb{Z}} \text{SW}_Z(-\kappa + i[T]) = 2n(\text{SW}_Z(-\kappa) + 0) = \pm 2n, \end{aligned}$$

where the sums in the middle of each equation reduce to a single term because $\pm\kappa$ are the unique basic classes of Z and must be linearly independent from $i[T]$ for $i \neq 0$ because $\kappa \cdot \kappa = K_Z \cdot K_Z > 0$ but $i[T] \cdot i[T] = 0$.

It follows that Z_n is distinguished from Z_m by its Seiberg-Witten invariants whenever $n \neq m$. Since $Z_n = M_{(0,2n,1)} \cup Q$ and $Z_m = M_{(0,2m,1)} \cup Q$, we conclude that $M_{(0,2n,1)}$ and $M_{(0,2m,1)}$ are distinct up to diffeomorphism rel boundary. \square

Proof of Theorem 1.4. By Proposition 4.11, the 4-manifold $M_{(0,2n,1)}$ is the branched cover of B^4 along S_n . Moreover, for all m , there is a natural identification of $\partial M_{(0,2n,1)}$ with $\partial M_{(0,2m,1)}$ arising from their identification with $\partial M = \Sigma_2(S^3, L)$. By Proposition 4.12, these 4-manifolds are distinct up to diffeomorphism rel. boundary whenever $m \neq n$. It follows that S_n and S_m are not smoothly isotopic rel. boundary in B^4 . \square

REFERENCES

- [AK80] Selman Akbulut and Robion Kirby. Branched covers of surfaces in 4-manifolds. *Math. Ann.*, 252(2):111–131, 1979/80.
- [Akb13] Selman Akbulut. Topology of multiple log transforms of 4-manifolds. *Internat. J. Math.*, 24(7):1350052, 14, 2013.
- [Akb16] Selman Akbulut. *4-manifolds*, volume 25 of *Oxford Graduate Texts in Mathematics*. Oxford University Press, Oxford, 2016.
- [Alf70] William R. Alford. Complements of minimal spanning surfaces of knots are not unique. *Ann. of Math. (2)*, 91:419–424, 1970.
- [Alt12] Irida Altman. Sutured Floer homology distinguishes between Seifert surfaces. *Topology Appl.*, 159(14):3143–3155, 2012.
- [Art26] Emil Artin. Zur isotopie zweidimensionalen flächen im \mathbb{R}^4 . *Abh. Math. Sem.*, pages 174–177, 1926.
- [AS70] William R. Alford and Christopher B. Schaefele. Complements of minimal spanning surfaces of knots are not unique. II. In *Topology of Manifolds (Proc. Inst., Univ. of Georgia, Athens, Ga., 1969)*, pages pp 87–96. Markham, Chicago, Ill., 1970.
- [BN05] Dror Bar-Natan. Khovanov’s homology for tangles and cobordisms. *Geom. Topol.*, 9:1443–1499, 2005.
- [CDGW] Marc Culler, Nathan M. Dunfield, Matthias Goerner, and Jeffrey R. Weeks. SnapPy, a computer program for studying the geometry and topology of 3-manifolds. <http://snappy.computop.org>.
- [CP20] Anthony Conway and Mark Powell. Embedded surfaces with infinite cyclic knot group. *Geom. Topol. (to appear)*, 2020.
- [Dai73] Roy J. Daigle. More on complements of minimal spanning surfaces. *Rocky Mountain J. Math.*, 3:473–482, 1973.

- [Eis77] Julian R. Eisner. Knots with infinitely many minimal spanning surfaces. *Trans. Amer. Math. Soc.*, 229:329–349, 1977.
- [FS97] Ronald Fintushel and Ronald J. Stern. Surfaces in 4-manifolds. *Math. Res. Lett.*, 4(6):907–914, 1997.
- [Gab86] David Gabai. Detecting fibred links in S^3 . *Comment. Math. Helv.*, 61(4):519–555, 1986.
- [Gom98] Robert E. Gompf. Handlebody construction of Stein surfaces. *Ann. of Math. (2)*, 148(2):619–693, 1998.
- [GS99] Robert E. Gompf and András I. Stipsicz. *4-manifolds and Kirby calculus*, volume 20 of *Graduate Studies in Mathematics*. Amer. Math. Society, Providence, RI, 1999.
- [HJS13] Matthew Hedden, András Juhász, and Sucharit Sarkar. On sutured Floer homology and the equivalence of Seifert surfaces. *Algebr. Geom. Topol.*, 13(1):505–548, 2013.
- [HKM⁺] Kyle Hayden, Seungwon Kim, Maggie Miller, JungHwan Park, and Isaac Sundberg. Ancillary files with the arXiv version of “Seifert surfaces in the 4-ball”.
- [HS21] Kyle Hayden and Isaac Sundberg. Khovanov homology and exotic surfaces in the 4-ball. *arXiv:2108.04810*, 2021.
- [HW92] Shawn R. Henry and Jeffrey R. Weeks. Symmetry groups of hyperbolic knots and links. *J. Knot Theory Ramifications*, 1(2):185–201, 1992.
- [Jac04] Magnus Jacobsson. An invariant of link cobordisms from Khovanov homology. *Algebr. Geom. Topol.*, 4:1211–1251, 2004.
- [JM18] András Juhász and Marco Marengon. Computing cobordism maps in link Floer homology and the reduced Khovanov TQFT. *Selecta Math. (N.S.)*, 24(2):1315–1390, 2018.
- [JPW14] Jesse Johnson, Roberto Pelayo, and Robin Wilson. The coarse geometry of the Kakimizu complex. *Algebr. Geom. Topol.*, 14(5):2549–2560, 2014.
- [Kak91] Osamu Kakimizu. Doubled knots with infinitely many incompressible spanning surfaces. *Bull. London Math. Soc.*, 23(3):300–302, 1991.
- [Kau72] Louis H. Kauffman. *Cyclic Branched Covers, O(n)-Actions and Hypersurface Singularities*. ProQuest LLC, Ann Arbor, MI, 1972. Thesis (Ph.D.)—Princeton University.
- [Kho00] Mikhail Khovanov. A categorification of the Jones polynomial. *Duke Math. J.*, 101(3):359–426, 2000.
- [Kho02] Mikhail Khovanov. A functor-valued invariant of tangles. *Algebraic & Geometric Topology*, 2:665–741, 2002.
- [Kho06] Mikhail Khovanov. An invariant of tangle cobordisms. *Trans. Amer. Math. Soc.*, 358(1):315–327, 2006.
- [Kir78] Rob Kirby. Problems in low dimensional manifold theory. In *Algebraic and geometric topology (Proc. Sympos. Pure Math., Stanford Univ., 1976), Part 2*, Proc. Sympos. Pure Math., XXXII, pages 273–312. Amer. Math. Soc., Providence, R.I., 1978.
- [Kir97] Rob Kirby. Problems in low-dimensional topology. In William H. Kazez, editor, *Geometric topology (Athens, GA, 1993)*, volume 2 of *AMS/IP Stud. Adv. Math.*, pages 35–473. Amer. Math. Soc., Providence, RI, 1997.
- [Kob89] Tsuyoshi Kobayashi. Uniqueness of minimal genus Seifert surfaces for links. *Topology Appl.*, 33(3):265–279, 1989.
- [Kob92] Tsuyoshi Kobayashi. A construction of 3-manifolds whose homeomorphism classes of Heegaard splittings have polynomial growth. *Osaka J. Math.*, 29(4):653–674, 1992.
- [Liv82] Charles Livingston. Surfaces bounding the unlink. *Michigan Math. J.*, 29(3):289–298, 1982.
- [LM97] Paolo Lisca and Gordana Matić. Tight contact structures and Seiberg-Witten invariants. *Invent. Math.*, 129(3):509–525, 1997.
- [LS22] Robert Lipshitz and Sucharit Sarkar. A mixed invariant of nonorientable surfaces in equivariant Khovanov homology. *Trans. Amer. Math. Soc.*, 375(12):8807–8849, 2022.
- [Lyo74] Herbert C. Lyon. Simple knots without unique minimal surfaces. *Proc. Amer. Math. Soc.*, 43:449–454, 1974.

- [MMS97] John W. Morgan, Tomasz S. Mrowka, and Zoltán Szabó. Product formulas along T^3 for Seiberg-Witten invariants. *Math. Res. Lett.*, 4(6):915–929, 1997.
- [Mor96] John W. Morgan. *The Seiberg-Witten equations and applications to the topology of smooth four-manifolds*, volume 44 of *Mathematical Notes*. Princeton University Press, Princeton, NJ, 1996.
- [MWW22] Scott Morrison, Kevin Walker, and Paul Wedrich. Invariants of 4-manifolds from Khovanov–Rozansky link homology. *Geom. Topol.*, 26(8):3367–3420, 2022.
- [Par78] Richard L. Parris. *Pretzel Knots*. ProQuest LLC, Ann Arbor, MI, 1978. Thesis (Ph.D.)–Princeton University.
- [Pla06] Olga Plamenevskaya. Transverse knots and Khovanov homology. *Math. Res. Lett.*, 13(4):571–586, 2006.
- [Rol76] Dale Rolfsen. *Knots and links*. Mathematics Lecture Series, No. 7. Publish or Perish, Inc., Berkeley, Calif., 1976.
- [Rud90] Lee Rudolph. A congruence between link polynomials. *Math. Proc. Cambridge Philos. Soc.*, 107(2):319–327, 1990.
- [SS64] Horst Schubert and Kay Soltsien. Isotopie von Flächen in einfachen Knoten. *Abh. Math. Sem. Univ. Hamburg*, 27:116–123, 1964.
- [SS23] Isaac Sundberg and Jonah Swann. Relative Khovanov-Jacobsson classes. *Algebr. Geom. Topol.*, 22(8):3983–4008, 2023.
- [Sza19] Zoltán Szabó. Knot Floer homology calculator. Available at <https://web.math.princeton.edu/~szabo/HFKcalc.html>, 2019.
- [The19] The Sage Developers. Sagemath, the Sage mathematics software system. Available at <https://www.sagemath.org>, 2019.
- [Tro75] Hale F. Trotter. Some knots spanned by more than one knotted surface of minimal genus. In *Knots, groups, and 3-manifolds (papers dedicated to the memory of R. H. Fox)*, pages 51–62. Ann. of Math. Studies, No. 84. 1975.
- [Vaf15] Faramarz Vafaee. Seifert surfaces distinguished by sutured Floer homology but not its Euler characteristic. *Topology and its Applications*, 184:72–86, 2015.
- [Wan22] Joshua Wang. The cosmetic crossing conjecture for split links. *Geom. Topol.*, 26(7):2941–3053, 2022.
- [Wil08] Robin T. Wilson. Knots with infinitely many incompressible Seifert surfaces. *J. Knot Theory Ramifications*, 17(5):537–551, 2008.
- [Zee65] Erik Christopher Zeeman. Twisting spun knots. *Trans. Am. Math. Soc.*, 115:471–495, 1965.

DEPARTMENT OF MATHEMATICS AND COMPUTER SCIENCE, RUTGERS UNIVERSITY–NEWARK,
NEWARK, NJ 07102 USA

Email address: kyle.hayden@rutgers.edu

DEPARTMENT OF MATHEMATICS, SUNGKYUNKWAN UNIVERSITY, SUWON 16419, REPUBLIC OF KOREA

Email address: math751@gmail.com

DEPARTMENT OF MATHEMATICS, STANFORD UNIVERSITY, STANFORD, CA 94305 USA

Email address: maggie.miller.math@gmail.com

DEPARTMENT OF MATHEMATICAL SCIENCES, KOREA ADVANCED INSTITUTE OF SCIENCE AND TECHNOLOGY, DAEJEON 34141, REPUBLIC OF KOREA

Email address: jungpark0817@kaist.ac.kr

MAX PLANCK INSTITUTE FOR MATHEMATICS, BONN 53111, GERMANY

Email address: isaacsundbe@gmail.com